Seep communities from two mud volcanoes in the deep eastern Mediterranean Sea: faunal composition, spatial patterns and environmental control

Bénédicte Ritt [1,2,*], Daniel Desbruyères [1], Jean-Claude Caprais [1], Olivier Gauthier [3], Livio Ruffine [1], Roselyne Buscail [4], Karine Olu-Le Roy [1], Jozée Sarrazin [1]

[1] Ifremer Brest, REM/EEP & REM/GM, Institut Carnot Ifremer-EDROME, BP 70, 29280 Plouzané, France
[2] Biology Department, Temple University, 1900 North 12th Street, Philadelphia, Pennsylvania 19122, USA
[3] IUEM, UBO, Technopôle Brest-Iroise, Place Nicolas Copernic, 29280 Plouzané, France
[4]CEFREM, CNRS, UMR 5110, Université de Perpignan, 52, avenue Paul Alduy, 66860 Perpignan, France

*: Corresponding author : benedicte.ritt@gmail.com

Abstract:
The Mediterranean Sea constitutes a unique environment to study cold-seep ecosystems due to the presence of different geodynamic settings, from an active margin along the Mediterranean Ridge (MR) to a passive margin in the Nile Deep-Sea Fan (NDSF). We attempted to identify the structure of benthic communities associated with the Napoli and Amsterdam mud volcanoes (MVs) located on the MR and to establish the links between faunal distribution and environmental conditions at different spatial scales. Comparison between the 2 MVs revealed that the faunal distribution seemed to be mainly controlled by the characteristics of the microhabitats. On both geological structures, the variability between the different microhabitats was higher than the variability observed between replicates of the same microhabitat, and the distribution of macrofauna was apparently linked to gradients in physico-chemical conditions. The peripheral sites from Napoli were generally more oxygenated and harboured lower species richness than the active sites. The reduced sediment microhabitat from Amsterdam presented the highest methane concentrations and was mainly colonised by symbiont-bearing vesicomyid bivalves and heterotrophic dorvilleid polychaetes. Overall, a higher taxonomic diversity was observed on Napoli. Substratum type was hypothesised to be the second factor influencing faunal distribution. The results of this study highlight the high heterogeneity of faunal communities associated with seep ecosystems within this region and the need to pursue investigations at various spatial and temporal scales.

Keywords: Mediterranean Ridge ; Cold seeps ; Benthic fauna ; Environmental conditions ; Diversity indices ; Microhabitats

1. Introduction

Cold seeps are geological features generated by mud, water and gas emissions occurring on the seafloor (Kvenvolden & Rogers 2005, Judd & Hovland 2007). Since their discovery on the Florida Escarpment in the Gulf of Mexico (Paull et al. 1984), more than 40 seep sites with chemosynthesis-based communities have been reported throughout the world"s oceans, at different depths (Sibuet & Olu 1998, Levin 2005, Campbell 2006). These sites are characterised by the formation of peculiar geological structures such as pockmarks, brine lakes, mud volcanoes or gas flares (Milkov 2000, Hovland et al. 2002, Levin 2005, Judd & Hovland 2007).

The Mediterranean Sea constitutes a unique environment to study cold-seep ecosystems due to the presence of different geodynamic settings, from an active margin along the Mediterranean Ridge (MR) to a passive margin in the Nile Deep-Sea Fan (NDSF). The eastern Mediterranean Sea is presently undergoing complex evolution due to the subduction of the African plate beneath the southern Eurasian plate. The MR is a particularly prominent morpho-structural feature along this major converging system. This large arc-shaped, accretionary wedge extends for more than 1 500 km in length and 200 to 250 km in width (Limonov et al. 1996). The presence of fluid seepages related to seabed structures along this ridge was first discovered south of Crete (Cita et al. 1981). Since then, mud diapirs and mud volcanoes (MVs) have been identified at several localities in the central MR (Cita & Camerlenghi 1990, Ivanov et al. 1996, Huguen et al. 2004), on the Anaximander Mountains (Woodside et al. 1998, Zitter et al. 2003), along the Florence Rise (Woodside et al. 2002, Zitter 2004), and in the Levant Basin (Coleman & Ballard 2001). The most recent investigations were focused on the NDSF, off the coast of Egypt, an area characterised by the presence of a heavily sedimented margin (Bellaiche et al. 2001, Mascle et al. 2001, 2006, Loncke et al. 2004). However, the first evidence of benthic communities based on chemosynthetic processes was found on the Napoli MV (Corselli & Basso 1996). It is now known that several of the MR sites (Salas & Woodside 2002, Olu-Le Roy et al. 2004, Werne et al. 2004) as well as those in the NDSF are colonised by various chemosynthesis-based faunal assemblages (Huguen et al. 2005, Zitter et al. 2005, Dupré et al. 2007, Ritt et al. 2011).

The first data on Mediterranean cold-seep communities were acquired during the French-Dutch MEDINAUT cruise (1998) in 2 regions: the Olimpi mud field and the Anaximander Mountains (Salas & Woodside 2002, Olu-Le Roy et al. 2004, Werne et al. 2004). These communities are dominated by small bivalves from 2 families (Mytilidae and Vesicomyidae) common to cold-seep environments (Duperron et al. 2009, Krylova & Sahling 2010, Olivier et al. 2011) and two others (Lucinidae and Thyasiridae) known from shallower sulphide-rich habitats including seeps (Dando & Southward 1986, Cary et al. 1989a, Olu-Le Roy et al. 2004, Brissac et al. 2011). Siboglinid polychaetes belonging to the clades Obturata (*Lamellibrachia anaximandri*, Southward et al. 2011) and Frenulata (*Siboglinum* sp.) as well as heterotrophic mega- and macro-faunal species have also been observed. The fauna seems to be concentrated at the summit of the MVs, where the seepage activity is usually the greatest, even in the brine lake zone on Napoli (Olu-Le Roy et al. 2004). Typical deep-sea taxa (fish, urchins, sponges) benefit from the increased biomass found near the seeps (Olu-Le Roy et al. 2004). The species richness of the symbiont-bearing fauna observed during the MEDINAUT cruise was much higher than that found in similar communities at comparable depths in other

oceans (Sibuet & Olu-Le Roy 2002). While environmental factors such as methane, sulphide or oxygen concentrations have been suggested as structuring factors in seep communities worldwide (Barry et al. 1997, Olu et al. 1997, Levin & Gage 1998, Sahling et al. 2002, Levin et al. 2003, 2010, Niemann et al. 2006, Olu-Le Roy et al. 2007, Cordes et al. 2010), those from the eastern Mediterranean Sea have been studied only recently (Ritt et al. 2010, 2011).

In 2007, various cold-seep ecosystems in the Mediterranean Sea were investigated during the MEDECO cruise. The present study aims to describe the structure of benthic communities associated with the Napoli and Amsterdam MVs located between 1940 and 2025 m depth on the MR and to establish the links between faunal distributions and environmental conditions at the microhabitat (several meters) to MV scale (several hundred meters). We aimed to understand the factors that influence the structure and diversity of seep communities in the Mediterranean Sea, using a mostly family-level taxonomic resolution.

2. Materials and methods

The first studies concerning the regions of interest were done during the MEDINAUT (1998), NAUTINIL (2003) and M70/3 (2006) cruises. Bathymetric maps and observations made during these cruises were used to decide on the dive strategy for the MEDECO cruise. The first leg of MEDECO took place from October 7 to 31 October 2007 on the R/V *Pourquoi Pas*? with the remotely operated vehicle (ROV) *Victor6000*. During this cruise, different deep-sea ecosystems of the Mediterranean Sea were visited, including the Napoli and Amsterdam MVs (Figure 1). Three dives, totalling 87 h of bottom time, were dedicated to sampling these 2 MVs.

2.1. Study area

2.1.1. Olimpi field – Napoli MV

The Olimpi field, located south of Crete (Figures 1a, b, c), is the largest known MV field on the MR. Its geomorphology has been extensively studied since its discovery in 1988 (Camerlenghi et al. 1992, Ivanov et al. 1996, Huguen et al. 2004). Most of the MVs found in this field are dome-shaped. Located at 1950 m depth, Napoli is among the largest MVs on Olimpi, reaching 1000 m across and 200 m high. It is surrounded by irregular mud flows and circular depressions (Figure 1b) and is characterised by the occurrence of fresh mud flows, brine pools, authigenic carbonate crusts (Huguen et al. 2005) and by intense degassing on its summit (Charlou et al. 2003). Two dives were entirely dedicated to sampling the macro- and meiofauna and characterising the environmental conditions at the immediate periphery of the centre (33°43.75′N – 24°40.95′E) at 1940 m depth.

2.1.2. Anaximander Mountains – Amsterdam MV

Located south of Turkey, the Anaximander Mountains are shaped by a complex of 3 MVs, rising more than 100 m above the seafloor, generally identified as conical topographic features to which the Amsterdam MV belongs (Zitter et al. 2005; Figures 1a, d, e). This MV, located at a maximum depth of 2040 m, is ellipse-shaped and reaches 3 km across and 100 m high. It has a very uneven terrain with depressions and abrupt

scarps, particularly on its summit, probably caused by an erupted mud flow of 300 m thickness (Woodside et al. 1998). The surface of Amsterdam is characterised by the presence of carbonate crusts, muddy areas and large rock clasts (i.e. rock fragments coming from deeper layers and expulsed to the seafloor with fluid and gas emissions). In contrast to the Napoli MV, no brine pools have ever been observed on this MV (Zitter et al. 2005) whereas carbonate crust associated benthic communities have been reported (Olu-Le Roy et al. 2004). Faunal sampling and environmental characterisation were performed during one long dive at 2 different sites located at the immediate periphery of the centre (35°20.10'N – 30°16.09'E; Figure 1d) at 2020 m depth.

2.2. Sampling sites

The 2 MVs harboured a mosaic of visually distinguishable microhabitats. Two of the sampled microhabitats were common to both MVs, were sampled: 1) brown sediments with high density of bivalve shells on the chaotic sediment surface (Biv, Figures 2a, g); and 2) carbonate crusts (CC, Figures 2c, i). The CCs presented different morphologies; they formed large and thick pavements on the sediment surface and also within sediments on Napoli, while they were more superficial and fragile on Amsterdam. The *Lamellibrachia* microhabitat (Lam) was only sampled on Napoli (Figure 2b). These Siboglinidae polychaetes were also observed on Amsterdam but they were located under CCc and were therefore difficult to sample. Bubble emissions were only observed on Amsterdam reduced sediments, constituting the reduced sediment microhabitat (Red, Figure 2h) located in a depression. On Napoli, additional samples were taken in the periphery of the *Lamellibrachia* microhabitat (Plam, Figure 2d) as well as at the periphery of the CC microhabitat (Pcc, Figure 2e) in settings resembling the Biv microhabitat. These sites were sampled to determine possible gradients between active (Lam, CC) and peripheral (Plam, Pcc) sites. These additional microhabitats were located from 2 to 22 m away from the active microhabitats (Table 1, Figure 1c). The so-called "active" microhabitats were those characterised by the presence of visible chemosynthetic fauna (e.g. *L. anaximandri*), specific geological features (e.g. CC) or seepage activity (e.g. bubble emissions or black sediments). The peripheral samples were taken on the edge of the active areas on the MVs and were distinct from the reference samples. On Napoli, the "active" sites and their peripheries were included within a 30 m diameter circle localised approximately 250 m away from brine evidences and 500 m from the central brine lake. On Amsterdam, Biv and Red were very close to each other (i.e. ~17 m) and separated by 300 m from the CC microhabitat (Figure 1e). Finally, the reference samples *sensu stricto* (Ref) were collected outside of each MV, a few thousand metres from the centre, and away from any seepage activity (Figures 1b, d). Contrary to the microhabitats on the MVs, 1 unique replicate was sampled at each reference site using a box-corer launched from the surface.

2.3. Sampling procedures

Environmental characterisation of each microhabitat was conducted before faunal sampling to avoid any disturbance that could be caused by the latter. *In situ* measurements of total sulphides ($H_2S+HS^-+S^{2-}$) were performed with CHEMINI, a miniaturised deep-sea chemical analyser (Vuillemin et al. 2009). CHEMINI's sample inlet was deployed for 20 min above the organisms and as close as possible (1 to 2 cm) to the seafloor using the ROV manipulator arm. Water and sediment samples were then

taken for chemical analyses using the PEPITO water sampler and tube corers (30 cm long; 5.4 cm inner diameter), respectively. PEPITO collects water in 200 ml titanium bottles and sampled at the same locations as those chosen for the CHEMINI measurements. Sediment tube cores were split horizontally on board and porewater was extracted by centrifugation of each sediment layer (every 0.5 cm for the first 2 cm, then every cm until 10 cm and every 2 cm until the end of the core) to measure chloride and sulphate concentrations. Sampling details for each microhabitat, periphery and reference site are given in Table 1. Unfortunately, due to technical and time constraints, the CHEMINI chemical sampling could not be completed on Amsterdam (e.g. no sulphide analysis was made).

The epi- and endofauna were sampled with blade corers (200 cm^2) at all soft sediment sites (Figures 2a, b, d, e, g, h). The number of samples for each microhabitat varied, depending on the time and number of corers available during a particular dive (Table 1). Due to these limitations, endofauna in each reference site was only sampled with a single box core, triggered from the surface. On carbonate crusts, the ROV suction sampler was used to collect the epifauna (Figure 2i) before collecting pieces of carbonate with its manipulator arm (Figures 2c, i). Each crust sample was put in an individual sampling box (Table 1).

In addition to the systematic sampling within the microhabitats, 2 CALMAR benthic chambers (Caprais et al. 2010) were deployed on Napoli by the ROV manipulator arm; the first one was deployed above live *Lamellibrachia anaximandri* (CALMAR A, Figure 2f) and the second was deployed a few metres away on reduced sediments devoid of siboglinids (CALMAR B, not shown), identified as a peripheral site. These benthic chambers were equipped with 2 independent oxygen probes (Aanderaa optodes) and 6 water sampling units. The probes were used to measure *in situ* dissolved oxygen consumption by the fauna while the water samples were used to validate the oxygen data and to calculate carbon dioxide and methane emission fluxes.

2.4. Physico-chemical analyses

The 200 ml water samples from PEPITO were used to determine pH as well as methane, oxygen, sulphate and chloride concentrations (Table 1). Measurements of pH were performed on board with a pH-meter linked to a glass-electrode (Metrohm) after calibration performed at 25°C using NBS standard solutions at pH ~7 and ~9 (Metrohm refs. 6.230.110 and 6.307.120 respectively). Reproducibility of the method was ± 0.01 pH units. Methane concentrations were measured in the laboratory using the headspace technique coupled with a gas chromatography equipped with a flame-ionisation detector (error of 4%, see method in Sarradin & Caprais 1996). Dissolved oxygen concentrations (in water samples) were determined using the Winkler method (Winkler 1888) adapted for small volumes, with an error of 4%. Sulphate and chloride concentrations (in water samples as well as in porewater extracted from sediment slices) were measured using an ionic chromatograph on an isocratic system (DX 120 DIONEX). Intact cores with supernatant water were used for oxygen measurements. Chemical differences in average surface dissolved oxygen, methane, sulphate and chloride concentrations as well as pH between the 2 MVs were evaluated with Mann-Whitney tests. However, due to the small number of samples (n=3 for each microhabitat), statistical comparison at a smaller scale, i.e. between the 2 common microhabitat types (Biv and CC) was not performed because of insufficient power.

The water sampled by CALMAR was immediately collected upon recovery. Dissolved oxygen consumption was calculated as explained above for the PEPITO samples. Total dissolved inorganic carbon (DIC) was determined using infrared (NDIR) gas analyses (Kaltin et al. 2005) and methane was analysed using headspace gas chromatography (Sarradin & Caprais 1996). Fluxes were calculated from the slopes of the linear regressions obtained with oxygen, methane and carbon dioxide concentrations versus time (Caprais et al. 2010).

Oxygen profiles within interstitial water (tube cores) were obtained with a microsensor OX 100 coupled to a picoammeter (PA 2000, Unisense) and a micro-manipulator using profix data acquisition software (Unisense). The resolution of the sensor was < 200 µm. Kendall rank correlations (τ) were computed between mean sulphate and chlorinity profiles within Lam, Biv and P(lam+cc) microhabitats from Napoli. The characterisation of the chemistry within the sediments is detailed in Supplement 1: Results.

2.5. Descriptors of the organic matter in sediments

Total nitrogen, carbon and organic carbon concentrations (TN, TC and TOC, respectively) were measured using freeze-dried, milled, sediment sub-samples. Homogenised, weighed samples were analysed in an automatic CN-analyser LECO 2000, after acidification with 2N HCl (overnight, at 50°C) to remove carbonates prior to organic carbon analyses (Cauwet et al. 1990). Precision was about 2% for TOC and 0.3% for TN. Calcium carbonate content was calculated from mineral carbon (TC-OC) using the molecular mass ratio ($CaCO_3$:C = 100:12). Percentages of organic carbon from additional samples (footnote „a" in Tables 1 & 3) were analysed with a LECO WR 12 auto-analyser after sediment decarbonation with 6N HCl. These analyses were performed independently from organic matter (OM) characterisation.

The C:N ratio was estimated to determine the origin and degradation stage of OM. Total hydrolysable amino acids (THAA) were assayed by a colorimetric method on the fraction hydrolysed by 6N HCl for 16 h at 110°C. Absorption of the products resulting from the amino acid-ninhydrin reaction was measured at 570 nm using a Beckman spectrophotometer (precision of 15%; Stevenson & Cheng 1970). Total lipids were measured by a colorimetric method after extraction with a 2:1 (v:v) chloroform:methanol mixture. Absorption of the products was measured at 520 nm with a Beckman spectrophotometer (precision of 10%; Barnes & Blackstock 1973). Total carbohydrates (CarbH) were measured by a colorimetric method on the fraction hydrolysed by 3M H_2SO_4. Absorption of the products resulting from the anthrone-sulphuric acid reaction was measured at 625 nm using a Beckman spectrophotometer (precision of 8%; Brink et al. 1960). The biopolymeric fraction of OM calculated as the sum of carbohydrate, protein and lipid contents was used as an index of the potentially available fraction for benthic consumers (Fichez 1991). This fraction is hereafter called “bio-available OM” (Bio-av. OM).

2.6. Faunal sorting and identification

Sediments from blade corers were processed as described by Ritt et al. (2010, 2011), except for the Lam cores that could not be sliced due to the presence of *Lamellibrachia*

tubes on the whole length of the cores and were thus considered as a single slice. Furthermore, cores from the reference sites were split by sections to 10 cm depth. It would have been preferable to analyse the distribution up to ~20 cm to be comparable to the maximum depths obtained with the blade corers and also to get the best representation of the vertical distribution at these sites but due to different sampling strategies, we only had access to the first 10 cm, leading to a probable underestimation. A great proportion of the endofaunal biomass in background sediments can be found below 20 cm depth at certain deep-sea sites (Jensen 1992, Dando et al. 2008). In addition, because the 250 µm mesh used here is inadequate for meiofaunal sampling (which usually requires 32 µm to 62 µm mesh; Hessler & Jumars 1974, Thistle 2003, Van Gaever et al. 2006), we focused on macrofauna *sensu stricto* (>250 µm, Hessler & Jumars 1974). Any meiofaunal taxa such as Nematoda, Copepoda and Ostracoda were treated separately and are detailed in Supplement 1: Materials and methods. Taxonomic determination was achieved at the family level for most of the taxa except for Demospongia, Hexactinellida, Scyphozoa, Polyplacophora, Nemerta, Leptostraca, Echinoida, Terebellida and Nematoda.

The CC samples were processed as described by Ritt et al. (2011) to assess surface area and area-related indicators such as density (estimation of the number of ind. m^{-2}) and biomass. On the other hand, carbonates were not broken to collect potential endofauna, leading to a possible underestimation of faunal abundance.

2.7. Measurement of taxonomic diversity at different spatial scales

Within-microhabitat (α) and between-microhabitat (β) diversity were estimated for all microhabitats as previously described by Ritt et al. (2011). Organisms from the whole cores and from the carbonate crusts (i.e. endo- and epifauna) were considered for these community analyses.

2.7.1. Alpha-diversity

The α-diversity analyses were performed at the family level; undetermined families, individuals or larvae were removed from the dataset because of the probability that they belonged to a family already listed. This may have resulted in an underestimation of the taxonomic richness. However, there were 3 exceptions, including the “undertermined Gastropoda” found at the periphery of the *Lamellibrachia* microhabitat from Napoli and at the reference site from Amsterdam for which no other Gastropoda families were observed. There were also the “undetermined Sipuncula” and “Undetermined Tanaidacea”, both observed in the reference site of Napoli with no other families. We chose to slightly under-estimate the taxonomic richness rather than to over-estimate it.

Individual-based and sample-based rarefaction curves were computed as in Ritt et al. (2011): first with macrofaunal datasets for each microhabitat at both MVs and then, with pooled data excluding reference sites away from each MV, and separating the “active” from the peripheral sites on Napoli. Expected richness for an effort of 50 individuals (ES50) was used to compare microhabitat richness at a constant sampling effort. Commonly used diversity indices (e.g. richness, Shannon"s entropy, Gini-Simpson, Pielou"s evenness) as well as with a more robust intrinsic diversity-based ordering method were also used as described by Ritt et al. (2011) to evaluate the taxonomic (family) diversity.

2.7.2. Beta-diversity

Despite the modest number of samples, multivariate analyses were conducted to better illustrate the similarities and differences among faunal samples. The lowest available taxonomic level was used (mostly family level) to perform principal component analysis (PCA) and to calculate the Jaccard similarity (Jaccard 1901, Koleff et al. 2003) coefficient as described by Ritt et al. (2010, 2011). A Procrustean randomization test (Jackson 1995; Peres-Neto & Jackson 2001) was performed to compare the PCA results of the macro- and meiofaunal datasets. Canonical redundancy analyses (RDA) were then performed on macrofaunal abundance data at both MVs with an environmental matrix that included pH, oxygen, methane, sulphate and chloride concentrations at the sediment-water interface, as well as the presence or absence of carbonate concretions. Faunal data were Hellinger-transformed prior to PCA and RDA (Legendre & Gallagher 2001).

All analyses were performed in the R environment (R Development Core Team 2012). Rarefaction curves, diversity indices and diversity profiles were computed both with the BiodiversityR package (Kindt & Coe 2005) and functions in Gauthier et al. (2010). Multivariate analyses were carried out using the vegan package (Oksanen et al. 2012).

3. Results

3.1. Physico-chemical characterisation of microhabitats

3.1.1. Sediment appearance

Soft sediments sampled at both MVs ranged from muddy to sandy in appearance. The lengths of the blade cores varied from 10 to 21 cm depending on the nature of the substratum (Table 1). Biv, Plam and Pcc from Napoli and Biv from Amsterdam were characterised by a layer of brown sediments, clearly distinct from the black sediment layer below (Table 2).

3.1.2. Chemical characterisation of the sediment-water interface

Sulphide concentrations measured at the water-sediment interface were lower than the limit of detection (<0.1 µmol l^{-1}) at every microhabitat on Napoli; sulphide was not measured on Amsterdam. Values of pH in water samples varied from 7.99 to 8.08 on both MVs (Table 2).

Oxygen data at the sediment-water interface were available for both MVs. On Napoli, oxygen varied from 196.4 µmol l^{-1} above CC to 222.5 µmol l^{-1} above Lam whereas it ranged from 186.8 µmol l^{-1} above Biv to 202.2 µmol l^{-1} above CC on Amsterdam (Table 2).

The highest methane concentration at Napoli was found in the CC microhabitat where it peaked at 4.29 µmol l^{-1}, whereas it reached only 0.76 µmol l^{-1} in the soft sediment microhabitat (Lam3; Table 2). In contrast, the highest methane value on the Amsterdam MV was observed over soft sediments, reaching 12.45 µmol l^{-1} above Red1/Red2 and

only 0.60 µmol l^{-1} on the CC microhabitat. The value measured on Red1/Red2 was the highest measured at either MV (Table 2).

Sulphate and chloride concentrations at the sediment-water interface from Napoli and Amsterdam varied from 27.6 to 31.0 mmol l^{-1} and from 530 to 591 mmol l^{-1} respectively. The lowest values for both chemicals were observed in the Amsterdam Red microhabitat (Table 2).

No significant differences in pH or chloride concentrations were detected using Mann-Whitney *U* tests between the 2 MVs (W=87, p>0.05; W=115, p=0.19 respectively), but differences in oxygen, methane and sulphate concentrations were significant (W=156, p<0.01; W=925, p<0.05 and W=162, p<0.01, respectively).

3.1.3. Flux measurements

On Napoli, the results obtained on colonised sediments after 14h incubation with the benthic chamber CALMAR A above *Lamellibrachia anaximandri* siboglinids (n>25 ind.) indicated an oxygen uptake of 35 mmol m^{-2} d^{-1} and a carbon dioxide flux of 34 mmol m^{-2} d^{-1}. A methane flux of 3 mmol m^{-2} d^{-1} was also observed. In contrast, under CALMAR B, deployed on peripheral sediments (Plam; no visible fauna), the oxygen uptake was 13.5 mmol m^{-2} d^{-1} with a carbon dioxide flux of 11.2 mmol m^{-2} d^{-1}. The methane flux never exceeded 0.05 mmol m^{-2} d^{-1}.

3.2. Distribution of organic matter in sediments

The percentages of organic carbon in the sediments varied from 0.27% in the Napoli bivalve microhabitat to over 1.82% in the Lam microhabitat where it reached its highest values (Table 3). A similar trend was observed for total nitrogen (TN), with concentrations at least 3 times higher in the Lam microhabitats; the lowest values were found in the Napoli Ref site. Similarly, the concentrations of lipids, carbohydrates and amino acids were highest on Lam. On the other hand, the C:N ratio was higher at the Napoli Ref site and lowest in the Lam microhabitats (Table 3). On Amsterdam, the C:N ratio was only slightly higher in the Biv microhabitat compared to the Ref site (Table 3).

Overall, the Lam microhabitat from Napoli was the most enriched in organic matter with a bio-available proportion >37.7%, which is nearly twice that observed on Biv at both MVs (23.7% at Napoli and 26.9% at Amsterdam; Table 3). In general, most organic compounds decreased with sediment depth (0 to 10 cm). The C:N ratios in surface sediments varied from 8.6 (Lam 1; Napoli) to 12.7 (Biv1; Amsterdam) with a maximum of 17.5 on the Napoli reference site (Table 3). They were relatively constant with depth with the exception of a sharp decrease in the 1 to 3 cm slice due to the presence of a black layer of fine sediments enriched in nitrogenous compounds.

The Biv microhabitat from Amsterdam was more enriched in amino acids and lipids, but poorer in carbohydrates than the same microhabitat on Napoli. While the TN was in the same range, the C:N ratio and the proportion of bio-available OM were slightly higher on Amsterdam than on Napoli (Table 3). The proportion of carbonates in the sediments was higher on Napoli. Regarding the Ref site, organic carbon content was low (<0.65%) at both MVs, and OM in sediments of the Ref site of Napoli were extremely depleted, with

the highest C:N ratio associated with a low TN and the highest proportion of carbonates (47%; Table 3).

3.3. Macrofaunal community description

Overall, a total of 3167 (Biv, Lam, Pcc, Plam; Table 4, and see Tables S4, S5, S7 & S8 in Supplement 2) and 4 841 (Red, Biv; Table 4, and see Tables S6 & S9 in Supplement 2) individuals were sorted in soft sediment microhabitats from Napoli and Amsterdam, respectively (Ref sites excluded). Among these, the proportion of macrofauna *sensu stricto* was approximately 46% for both. In the CC microhabitats, a total of 286 and 111 individuals were sorted with a respective proportion of 65 and 51% of macrofauna *sensu stricto* (Table 1 in Supplement 1 and Tables S4 to S9 in Supplement 2). Relative macrofaunal abundances varied between microhabitats and between replicates of the same microhabitat on both MVs.

3.3.1. Abundance, density, composition and α-diversity

On Napoli active sites, the mean macrofaunal densities varied from 1607 ind. m^{-2} on CC to 3733 ind. m^{-2} in Lam sediments. Densities reached 2925 and 10688 ind. m^{-2} at the periphery of the Lam patches and CCs, respectively. Density was very low at the Ref site with 104 ind. m^{-2} (Table 5). Overall, on Napoli active seep sites (Biv, Lam, CC), the highest macrofaunal densities were found on Lam (Table 5).

On Amsterdam active sites, the mean macrofaunal densities varied from 1222 ind. m^{-2} in CC to 24700 ind. m^{-2} in Red. The density was very low at the Ref site reaching 232 indi. m^{-2} (Table 6). Overall, on Amsterdam active seep sites (Biv, Red, CC), the highest macrofaunal density was found in Red (Table 6).

Disregarding the Ref sites, the lowest macrofaunal densities were observed in CC on both MVs while the highest was observed in the Red microhabitat on Amsterdam, with a density representing up to 6 times the highest density on Napoli active sites (24700 vs. 3733 ind. m^{-2} (Lam); Tables 5 & 6). Macrofaunal densities were much higher within soft sediment microhabitats on Amsterdam than on Napoli (Tables 5 & 6).

The rarefaction curves on macrofaunal data for each microhabitat on both MVs showed high variability in terms of diversity and adequacy of sampling effort (Figure 3). The fact that the curves do not level off indicates that, with the exception of Pcc, most Napoli microhabitats were under-sampled (Figure 3a). Nonetheless, the Biv microhabitat appeared to have the richest, and the Pcc microhabitat had the poorest communities sampled on Napoli (Figure 3a, Table 5). It should be noted that additional sampling could change the ranking of the curves (Figure 3a). Most communities, and in particular the Ref site and CC microhabitats, had high evenness while the periphery of the CC was notably uneven (*J'*; Table 5). Moreover, the CC microhabitat was almost 4.5 times more diverse than its periphery ($Exp[H_e']$; Table 5).

On Amsterdam, and because of the high density, Red was the only habitat that showed a leveled-off curve (Figure 3b). The curves and the low numbers of captured individuals for Biv, CC and Ref indicate that these microhabitats were under-sampled; especially the CC that had the lowest observed taxonomic richness (S_{obs}). The observed macrofaunal family richness (S_{obs}) in Red, CC and Ref was between 10 and 12, although it reached

25 in Red, but ES50 in Red was much lower (13; Table 6) and additional samples should confirm this ranking (Figure 3b). As it was observed on Napoli, the highest richness was observed in the Biv microhabitat (Figure 3b). The evenness (*J'*) was higher at Ref and in Biv and lowest in Red. The Shannon and Simpson indices gave the exact same ranking: they were highest in Biv, intermediate in Ref and CC and lowest in Red (Biv>Ref>CC>Red; Table 6) and according to the number equivalents of the Shannon index, Biv was almost 4 times more diverse than Red (Table 6). At both MVs, the evenness was higher at the Red sites (Tables 5 & 6).

To compare the 2 MVs (Napoli and Amsterdam), we pooled the data from all microhabitat samples (Ref sites excluded). The sample-based rarefaction curves on macrofaunal data from pooled microhabitats clearly showed that the active sites of Napoli exhibited the highest diversity while the picture was less clear for the peripheral sites and Amsterdam active sites (Figure 4a). The curves for the Amsterdam active sites and the peripheral sites on the Napoli provide a relatively good picture of their macrofaunal taxonomic richness, but it is unclear which of the 2 harbours higher taxonomic richness (Figure 4a). Despite a lower sampling effort (9 versus 17), higher macrofaunal densities led to more individuals were observed on Amsterdam than on Napoli.

Of the taxa present, different morphologies may be distinguished among Demospongia, Terebellida, Leptostraca and Nematoda, whereas a single morphology was observed for Hexactinellida, Scyphozoa, Polyplacophora, Nemerta and Echinoida suggesting the presence of a single family for these taxa. On Napoli, Biv was dominated by Paraonidae polychaetes (24.5% of the total abundance; Table 4), Demospongia (~7%) and Orbitestilidae gastropods (4.9%). The Obturata polychaetes dominated in Lam microhabitat (25%) while CC was dominated by Porifera (~27%; Table 4). Macrofaunal communities at the periphery of Lam and CC were mainly represented by Paraonidae polychaetes (17.1%) and Agathotanaidae (65.5%; Table 4). The Napoli Ref site was dominated by Spionidae polychaetes (19.2%) and several other families in equal proportion (7.7%; Table 4). It is interesting to note that most polychaete families observed in Biv were absent in Lam and *vice versa*. Indeed, the 2 siboglinid species never co-occurred in a given microhabitat (Table 4). For the peripheral samples, replicates showed higher heterogeneity between replicates taken close to the active sites (Plam-A and Pcc-A) than between those taken farther away (Plam-B and Pcc-B; Table 4). Overall, most of the families were common (8) to both active and peripheral sites from Napoli (Table 4). Five families were common to both active sites and the Ref site, and a single family was exclusively observed at the latter (Scalibregmatidae; Table 4).

On Amsterdam, Paraonidae polychaetes dominated Biv (22.3% of the total abundance; Table 4) while Serpulidae represented 52.6% of the total macrofauna in CC. Red was dominated by undetermined Vesicomyidae bivalves with a proportion close to 61.3% (Table 4) while Chrysopetalidae polychaetes dominated the Ref site (51.8%, Table 4). Similar to what was observed on Napoli, the 2 siboglinid species appeared to segregate according to microhabitat, with *Siboglinum sp.* being present exclusively in the Biv microhabitat and *Lamellibrachia anaximandri* only in CC (Table 4). Interestingly, 5 of the 8 polychaete families present at the Ref site were not observed at any of the active sites (Table 4).

When comparing the 2 MVs, it can be noted that poriferans and cnidarians were exclusively observed on Napoli, gastropods had higher occurrences on Napoli and bivalves were more represented on Amsterdam. The microhabitats Lam on Napoli and Red on Amsterdam were both characterised by the presence of reduced sediments from the surface to the deeper layers, by low oxygen penetration in Lam and one of the lowest oxygen concentrations in Biv, and by the presence of dorvilleid and terebellid polychaetes (Table 4).

The right tail-sum intrinsic diversity profiles for the pooled samples confirmed that Napoli had the highest α-diversity (Figure 4b). On the Amsterdam MV, the most abundant taxa represented 50% of the total macrofaunal abundance, but only 10% on Napoli (Figure 4b). Assuming homogenous spatial distribution on each MV and that all available microhabitats were sampled, additional sampling would probably not change the diversity ordering of these MVs. However, we know that all microhabitats were not sampled and that seep communities tend to have heterogeneous spatial distributions; it is thus likely that our estimates do not give a complete picture of the diversity of these 2 MVs.

3.3.2. Macrofaunal biomass

The highest biomass was observed on Napoli, in the Lam microhabitat (up to 4 kg wet weight [ww] m^{-2}; Table 5) due to the presence of long (up to 1 m) Siboglinidae polychaetes. In the other Napoli microhabitats, biomass was low, not exceeding 0.019 kg ww m^{-2} (Table 5). On Amsterdam, the mean biomass was more homogeneous throughout the microhabitats, ranging from 0.0012 to 0.049 kg ww m^{-2} (Table 6). Apart from the high values observed in the Napoli Lam microhabitat, the mean biomasses observed in the Amsterdam MV microhabitats were generally higher than those observed on Napoli. The vertical distribution of the biomass is presented in Section 2 and Figure S2 of Supplement 1.

3.3.3. Symbiont-bearing fauna versus heterotrophic fauna

The symbiont-bearing fauna (SBF) represented from 0 to 77% of the total macrofaunal abundance sampled on the 2 MVs (Tables 5 & 6; Figure 5). The SBF observed in the microhabitats sampled on Napoli was dominated by siboglinid polychaetes, whereas on Amsterdam, it was dominated by various bivalve families, especially Vesicomyidae (Table 4). On Napoli, Siboglinidae were represented by 2 main groups: the vestimentiferans or obturates (*Lamellibrachia anaximandri*) that were exclusively observed in the Lam microhabitat and the frenulates (*Siboglinum* sp.), that were exclusively found in the Biv microhabitat (Table 4). Live *L. anaximandri* were observed on Amsterdam, often associated with CCs, but were not sampled (Table 4).

On both MVs, the CC microhabitat exhibited the lowest proportion of SBF (up to 3.7% on Napoli and up to 9.1% on Amsterdam; Tables 5 & 6) with only two-thirds of the samples containing SBF. Densities of SBF were higher in Lam on Napoli and in Red on Amsterdam, with a dominance of siboglinid polychaetes in the former and vesicomyid bivalves in the latter (Figure 5). Although the highest SBF densities were associated with the highest methane concentrations on Amsterdam (Red), the opposite pattern was observed on Napoli where the highest concentrations above CC were rather associated with the lowest SBF densities (Figure 5).

3.3.4. Beta-diversity patterns

Macro- and meiofaunal from both MVs did not exhibit the same β-diversity patterns (Procrustes test m_{12}=0.274, p=0.538 for Napoli and m_{12}=0.459, p=0.201 for Amsterdam and 1000 permutations). It cannot be ruled out that these differences are attributable to the sampling strategy; thus we decided to focus on macrofauna *sensu stricto* thereafter.

On Napoli, mean Jaccard"s similarities for macrofauna were systematically lower than 40% within the same microhabitats (Table 6), implying a certain degree of heterogeneity at the microhabitat scale. PCA and clustering of macrofaunal abundances data allowed the distinction of 3 groups: Biv and CC microhabitats; Plam and Pcc microhabitats; and the Lam microhabitat. Overall, variability was lower within- than among microhabitat (Figure 6a). Of the taxa that contribute to the dispersion of samples in the PCA, Demospongia, Orbitestillidae and Scyphozoa were more abundant in Biv and CC, Obturata in Lam, and Agathotanaidae and Paraonidae in the peripheral microhabitats (Figure 6a).

Similarly, variability was higher among microhabitats on Amsterdam (Figure 6c). PCA and clustering allowed the identification of 3 groups (Figure 6d). Within microhabitats variability was lower than at Napoli, with a mean of up to 55% shared species in the Red microhabitat (Table 6). Of the taxa that contribute to the dispersion of samples in the PCA, Serpulidae polychaetes dominated CC samples, while Vesicomyidae bivalves were relatively more numerous in Red (Figure 6c).

When considering samples from both MVs, Red from Amsterdam appeared clearly distinct from all the others and showed high homogeneity between replicates (Figures 6e, f). Among the remaining microhabitats, CC from both MVs made up a second group with Lam and Biv from Napoli, whereas the peripheral microhabitats from Napoli and Biv from Amsterdam constituted a third group that also include the Ref sites (Figures 6e, f). Of the taxa that contributed to the dispersion of samples in the PCA, Vesicomyidae and Dorvilleidae had high relative abundances in the Red microhabitat from Amsterdam but were nearly absent from all other samples (Figure 6e, Table 4). Serpulidae, Orbitestellidae and Demospongia were most represented in the microhabitats of the second group (Figure 6e). Finally, Paraonidae, Cirratulidae and Agathotanaidea had higher relative abundances in the microhabitats of the third group (Figure 6e).

The RDA performed on macrofaunal abundances of all microhabitats from both MVs explained 56.4% of the variance in taxonomic distribution (pseudo-F=6.26, p<0.001; Figure 7). With the exception of pH, the other quantitative explanatory variables (oxygen, sulphate, methane and chloride) were mostly related to the first axis. Methane and pH were negatively correlated to oxygen, chloride and sulphate concentrations. PH and chloride explained some of the variations on the second axis, as did the presence/absence of carbonates, underlining the important distinction between hard (Co) and soft (Sed) substrata. The Red microhabitat on Amsterdam, with a high contribution of Dorvilleidae and Vesicomyidae, was the most methane-rich and was differentiated from all other microhabitats. On the other hand, the Napoli peripheral sites as well as the Amsterdam Biv microhabitat with high oxygen/high sulphate concentrations. The distribution along the second axis shows that the CC microhabitats on both MVs were close to Biv on Napoli and also to Lam. Taxa related to the lower part of the second axis such as Demospongia and Serpulidae are typical sessile fauna observed on hard substrata. Peripheral microhabitats as well as the Biv microhabitat on

Amsterdam were grouped along the second axis, primarily under the influence of the presence of soft substrata (Figure 7).

4. Discussion

The cold seeps located along the MR are characterised by a high number of MVs and spectacular fluid emissions on the seafloor. Napoli and Amsterdam are 2 examples of active MVs that can be distinguished by the presence of brine lakes, mud flows, chaotic centres and visible fauna at their peripheries. Both MVs are located on an active margin, in the same range of depths at ~2000 m and exhibit similar types of microhabitats, such as sediments covered by bivalve shells, reduced sediments and carbonate crusts.

In this study, most of the investigations focused on the centre of both Napoli and Amsterdam MVs. The variety of visually distinguishable habitats reflects the high spatial variability of fluid intensity on their surfaces. These visual features represent potentially different microhabitats in terms of chemical environment and faunal composition. The Napoli MV is characterised by the presence of brines due to the upward migration of fluids enriched by Messinian salt deposits (Charlou et al. 2003). Amsterdam, however, is characterised by the presence of gas hydrates (Lykousis et al. 2008). Based on the temperature gradients measured within the sediments in their centre, Amsterdam (36°C at 6 m below the seafloor) has a higher activity than Napoli (14.9°C measured at 10 m below the seafloor; JP Foucher, pers. comm.). This is also supported by the highest methane concentrations that reach up to 12.45 µmol l^{-1} (Red) at Amsterdam"s surface. Brine fluids also represent a major source of methane on Napoli"s surface. Methane concentrations found in both MVs reach at least 3 orders of magnitude higher than in the background ($0.4x10^{-3}$ µmol l^{-1}; Charlou et al. 2003) and sustain faunal communities having densities 2 orders of magnitude higher than the reference sites. Chemical and sediment instability induced by brines on Napoli prevent the establishment of faunal communities throughout this active region therefore restrincting them to peripheral areas.

4.1. Community structure at the MV scale: Napoli

The first structuring factor of the faunal distribution among microhabitats on Napoli appears to be the chemical gradients (methane, oxygen, sulphate and chloride), which are themselves related to the fluid intensity. The second factor appears to be the type of substratum (hard or soft).

Above the CC microhabitat, which appeared to be the most constraining microhabitat on Napoli, the high methane concentration (4.3 µmol l^{-1}) was associated with the lowest oxygen concentration (196.4 µmol l^{-1}) encountered. Despite the lack of flux rate measurement above CC, methane concentrations at the interface suggest an active area of fluid emissions in spite of the thick carbonate pavement. The Lam microhabitat had methane concentrations 5.6 times lower (0.76 µmol l^{-1}) than CC, but estimated flux rates measured in Lam (from 9.3 to 63 cm yr^{-1}) confirmed that Lam undergoes high upward fluid fluxes. In terms of fauna, different communities inhabited CC and Lam, partly related to the type of substratum. Indeed, sessile heterotrophic taxa, such as Porifera, Actiniaria and Gastropoda dominated the CC community, while *Lamellibrachia anaximandri* living with thiotrophic bacteria were the most represented taxa in Lam in

terms of density and biomass. Only the first centimetres of *L. anaximandri* were visible on the seafloor, while their tubes were deeply anchored within reduced sediments and may reach at least 20 cm in depth for the longest individuals (B. Ritt, pers. Obs.). They probably have access to sulphides by their posterior end (Julian et al. 1999) to fuel their endosymbionts as observed in Siboglinidae bushes in the Gulf of Mexico (Bergquist et al. 2002). Therefore, the non-detection of sulphides at the sediment surface does not preclude their production within sediments. Furthermore, the presence of *L. anaximandri* corroborates the hypothesis of the sulphide production within sediments to sustain its symbionts. This species is ubiquitous in the Mediterranean seeps and relies on sulphides for its survival (Olu et al. 2004; Southward et al. 2011).

Despite a potential bias induced by the sampling strategy used on CC (i.e. small surface sampled, under-representation of the total fauna), diversity (richness and evenness combined) and family richness (ES50: 17 in CC versus 10 in Lam) were higher at CC than Lam. These results contradict our expectations since we had assumed we would observe lower diversity in environments with higher constraints. Indeed, CC seems to provide various ecological niches for both symbiotic and heterotrophic fauna. Likewise, it appears that the environmental conditions in Lam do not enhance its faunal diversity, but contrarily, favour colonisation by a few specialised symbiotic species and heterotrophic species adapted to high amounts of OM, low oxygen penetration (few millimetres) and high upward fluxes. The Lam microhabitat may constitutes a complex system associating chemical and biological reactions with advection-diffusion processes highly variable between replicates (located 1 to 2 m away), and as constraining as CC. This is exemplified by the wide range of estimated flux intensity (from 9.3 to 63 cm yr^{-1}) and the heterogeneity of sulphate and chloride profiles that reveal multiple fluid origins (i.e. seawater, fresh water, brine). The high concentrations of organic carbon (up to 1.82% of organic carbon), which are higher than those recorded in sites without seepage and at the same depth in the Mediterranean Sea (from 0.30 to 0.69% of organic carbon; Buscail & Germain 1997, Danovaro et al. 1999), corroborate the hypothesis of high local production and turnover of OM.

The Biv microhabitat appears to have weaker fluid intensity with methane concentrations 1.5 times lower than Lam. The seepage activity at the microhabitat is also indirectly evident by the presence of *Siboglinum* sp. frenulates. This dominant Siboglinidae sub-family lives with sulphur-oxidising bacteria and probably also methane-oxidising bacteria (Bright & Giere 2005, Dubilier et al. 2008, Rodrigues et al. 2011). At our study sites, the siboglinid sub-families Frenulata and Obturata, did not co-occur in the same microhabitat, suggesting that they may require distinct environmental conditions. In fact, *Lamellibrachia anaximandri* appears to tolerate higher fluid fluxes than *Siboglinum* sp. However, Southward et al. (2011) observed co-occurrence at both MVs. This may suggest that the environmental conditions of our sampling sites may be more contrasted than those sampled previously by Southward et al. (2011). In addition to the presence of SBF, stable isotope signatures of the sedimented OM sampled at the summit of the Napoli MV confirm the presence of methane-influenced sediments (~36‰; Carlier et al. 2010). These signatures also suggest the influence of phytoplankton in the food web (~22‰; Carlier et al. 2010). In terms of environmental conditions, Biv may be considered an intermediate microhabitat. For the fauna, Biv is close to CC due to common taxa, such as Porifera, Actiniaria and Scyphozoa, which may use the empty bivalve shells as hard substrata to colonise.

The peripheral microhabitats of Lam and CC were characterised by some of the highest oxygen concentrations (up to 221.4 µmol l-1 in Plam). Peripheral microhabitats were sampled to determine possible gradients between active (Lam, CC) and peripheral (Plam, Pcc) sites on Napoli. Only slight differences in terms of methane and oxygen concentrations were observed between Lam and Plam with values respectively reaching 0.76 and 222.5 µmol l-1 in the former and up to 0.56 and 221.4 µmol l-1 in the later. However, they present important differences in advection rates, which were close to 0 in Plam suggesting a lower input of methane and sulphides. As a result, both Lam and Plam were located at the opposite side of the chemical gradient and were inhabited by distinct communities. Indeed, Plam was dominated by Paraonidae polychaetes, a dominant family in benthic communities of deep, sandy or silty areas (Rouse & Pleijel 2001), while Lam was dominated by the symbiont-bearing Lamellibrachia anaximandri. Concerning CC and Pcc, their spatial proximity was apparently their only common feature since there was an obvious heterogeneity in methane concentrations that are up to eight times higher above CC (4.29 µmol l-1) than above Pcc (0.50 µmol l-1). To summarize, on Napoli the peripheral sites appear to be distinct from the active sites with their relatively mild abiotic conditions that have favored high macrofaunal densities, particularly in Pcc (up to 10688 ind. m^{-2}). Considering all microhabitats from the 2 MVs, the peripheral sites from Napoli appeared to present the mildest environmental conditions. Additional sampling may be useful to acquire better knowledge of the chemical gradients occurring between active and peripheral sites and to assess the relevance of the "active" and "peripheral" labels, which were primarily based on visual observations.

4.2. Community structure at MV scale: Amsterdam

Similarly to Napoli, faunal distribution among microhabitats on Amsterdam appeared to be related to the chemical gradients (methane, oxygen, sulphate and chloride). The influence of the type of substrate also seemsed to be the second structuring factor.

The Red microhabitat was by far the most constraining microhabitat on Amsterdam with low oxygen concentrations (188.2 µmol l^{-1}) and methane concentration reaching 12.45 µmol l^{-1}. These values were the highest measured in this study, reaching nearly 3 times the concentrations observed on Napoli (CC). Red presented a wide range of methane concentrations highlighting the heterogeneity of the fluid intensity at sa mall spatial scale (metres). As expected, faunal richness was lower in Red than in Biv (ES50: 4 versus 13 respectively). The highly constraining conditions (i.e. low oxygen) favour the establishment of high densities of symbiont-bearing vesicomyids, probably juveniles of *Isorropodon perplexum.* This species lives with sulphur-oxidising bacteria and is ubiquitous in both eastern Mediterranean Sea seep sites and the Marmara Sea (Olu-le Roy et al. 2004, Ritt et al. 2010).

In terms of environmental conditions, the CC and Biv microhabitats presented slight differences. CC appeared more oxygenated (up to 202.2 µmol l^{-1} versus 195.5 µmol l^{-1} in Biv) and less enriched in methane than Biv (up to 0.60 µmol l^{-1} in CC compared to 0.70 µmol l^{-1} in Biv). Nevertheless, despite their mild environmental conditions, the presence of SBF (*Siboglinum* sp., *Lucinoma kazani*, *Thyasira striata* and undetermined vesicomyids) in CC and Biv suggests the presence of seepage activities in both microhabitats. The family richness on CC was lower than expected considering that the environmental conditions are less constraining than in Red. CC, however, presented a

family richness higher than that of Red (ES50: 9 in CC versus 4 in Red). Here again, the bias introduced by the sampling strategy may explain these unexpected results and limit our conclusions about the CC microhabitat. Regardless of the possible under-estimation of the faunal community on CC, some trends can still be observed. There, the fauna is mainly represented by the Serpulidae polychaetes. Biv appears to encompass abiotic conditions that favour relatively high densities and a slightly higher richness (ES50: 13) and an observed family richness twice as important as that from other Amsterdam microhabitats (S_{obs}: 25). Additional investigations are needed to understand which parameters drive this relatively high diversity in Biv.

4.3. Comparison at the scale of the Mediterranean Ridge

In terms of global activity, the Amsterdam MV appears to be more active and unstable (Charlou et al. 2003) and constitutes a more constraining environment for faunal colonisation than the Napoli MV. At both MVs, high heterogeneity was observed not only between the different microhabitats but also between replicates of the same microhabitat. The distribution of microhabitats on these 2 MR MVs, however, suggests that the type of habitat controls the structure of seep communities, rather than the geographical location as observed at the NDSF sites (Ritt et al. 2011). In terms of fauna, Napoli appeared to harbour higher taxonomic richness at the family level than Amsterdam. Nevertheless, faunal densities on Amsterdam were 2.3 times higher than on Napoli. This suggests more stringent environmental constraints in Amsterdam microhabitats, characterised by high methane and low oxygen concentrations.

This study also suggests that the substratum type is the second structuring factor of the faunal composition and distribution. The CC microhabitat, however, appeared highly heterogeneous within and between sites. Indeed, CC at both MVs presented different morphologies (Aloisi et al. 2000, Aloisi et al. 2002) and variable proportions of aragonite, dolomite and calcite (Pierre et al. 2008, 2010). Furthermore, results from CC microhabitats at both MVs must be interpreted in consideration of (1) an insufficient sampling effort to get a complete picture of the community, and (2) no direct sampling of the crust endofauna. Despite these caveats, the CC microhabitats presented unexpectedly high taxonomic richness for harsh environmental conditions and additional samples would probably not change this trend. The study of the CC communities appears to be complex due to the difficulties encountered during sampling and the inherent characteristics of the carbonates. Indeed, the different morphologies of CCs may be considered as different stages of formation that are related to variations in seepage activity and fluid composition. It could be interesting to further investigate the faunal composition on these different carbonate morphologies to determine whether the carbonate composition influence the faunal composition.

4.4. Comparison at larger scales

Overall, among the seep sites studied in the Mediterranean Sea, the Red and CC microhabitats are commonly found (Ritt et al. 2010, Ritt et al. 2011). Each microhabitat, however, seems unique with regard to its faunal composition, the proportion of SBF and the taxonomic richness at the family level. Similar *Lamellibrachia* aggregates anchored in reduced sediments have been observed in the NDSF (B. Ritt, pers. Obs.), but no Siboglinidae polychaetes have been observed in the Marmara Sea so far. Lam from

Napoli presents similarities with the reduced sediments from the Amon MV in the eastern Province of the NDSF (1000 m depth) where the SBF is represented by Siboglinidae from both sub-families as well as by Mytilidae (Ritt et al. 2011). Similarly, the reduced sediments from Amsterdam were dominated by the vesicomyid *Isorropodon perplexum* as observed in the reduced sediments from the Pockmark area in the central province of the NDSF. Sulphide concentrations within Napoli and Amsterdam sediments were not available in this study, but when considering the SBF, we can expect that (1) as in the NDSF sites, sulphides are produced within Lam and Red from Napoli and Amsterdam respectively, and, (2) the fluid flow on Amsterdam may be higher than on Napoli. Indeed, sulphide concentrations reached 2.5 mmol l^{-1} at 5 cm depth at Amon, while 25 mmol l^{-1} was recorded at the Pockmark area where the fluid flow intensity was assumed to be higher (Ritt et al. 2011).

Once more considering the SBF, the CCs from Napoli and the Marmara Sea present the same dominant taxa including Mytilidae and some sessile taxa, such as Porifera and Cnidaria. The carbonates from the Marmara Sea also form thick pavements, which do not appear to prevent methane fluid and sulphide diffusion to fuel the dense community of sulphur-oxidising Mytilidae (Ritt et al. 2012). This observation suggests that the presence of a thick pavement is not necessarily associated with past activity. The high methane concentrations above CC on Napoli corroborate this theory. However, the CCs from Napoli and the Marmara Sea differ from those from Amon, which are devoid of SBF and are likely located in an area of low fluid influence area (Dupré et al. 2007; Ritt et al. 2011). As stated earlier, the carbonate composition related to the seepage activity seems to be a potential structuring factor that needs further investigation.

In terms of chemistry, methane and oxygen gradients showed opposite trends and appeared to be important structuring factors. This was also the case for symbiont-bearing species (Olu-Le Roy et al. 2007) and associated heterotrophic polychaetes (Menot et al. 2010) in the giant REGAB pockmark in the Gulf of Guinea. Substratum type is also an important parameter observed at REGAB, influencing the spatial distribution of siboglinids and vesicomyids (Olu-Le Roy et al. 2007). Napoli MV shares similarities with cold seeps of the Gulf of Mexico (Cary et al. 1989b, MacDonald et al. 1990) since it is under the influence of salt-saturated brine lakes and upward brine migration fuelled by salt deposits (Cita & Ryan 1973, Hsu et al. 1977). However, estimated advection rates of upward fluxes on Napoli (from 9.3 to 63 cm yr-1) are much higher than those estimated for the Gulf of Mexico (0.2 and 3.2 cm yr-1; MacDonald et al. 1993, MacDonald et al. 2000). The brine lakes of Napoli, located at the centre of the MV where the activity appears high, are characterised by high salinity (82‰) and elevated chloride concentration (1380 mmol l-1; Charlou et al. 2003). Similar brine lakes have been observed in the western province of the NDSF, especially on Cheops and Chefren MVs at 3000 m depth. These MVs are characterised by the presence of high methane concentrations and salinity above the brines that are higher than on Napoli (Huguen et al. 2009). Brine seepage appears to induce sedimentary instability and to create local spots of activity, similar to what is observed in the Lam microhabitat on Napoli. No brines were observed on Amsterdam but instability may be created by mud flows (Zitter et al. 2005) such as those detected on the Håkon Mosby MV on the Norwegian margin (Feseker et al. 2008). This well-studied MV undergoes episodic mud eruptions that generate sedimentary and chemical instability, influencing the distribution of the benthic fauna in concentric belts around the summit (Jerosch et al. 2007). At the Napoli and Amsterdam MVs, the visible fauna is located on particular microhabitats on their active summits but not necessarily associated with dynamic structures such as brines or mud

flows (Olu-Le Roy et al. 2004, Zitter et al. 2005). Further investigations are needed to enhance our understanding of the faunal distribution on Napoli and Amsterdam MVs. Extending the sampling protocol to other MVs in the Olimpi Field and the Anaximander Mountains should further increase our understanding of regional distribution patterns and how they are linked with larger-scale processes. Furthermore, meio- and macrofauna appear to be differently influenced by the nature of the microhabitat and underlying physico-chemical factors but this may be attributable to the incomplete sampling of meiofauna during this study. Further investigations, focusing on meiofauna with an appropriate sampling strategy, may determine whether this faunal compartment behaves in the same way in relation to the conditions of the environment as the macrofauna.

Acknowledgments

The captain and crew of the R/V *Pourquoi pas?* as well as the pilots of the ROV *Victor6000* are warmly acknowledged for their dedicated assistance and for contributing to the success of the MEDECO cruise. The chief scientist of this cruise leg 1 (2007) was J.S. The faunal samples were identified by an international network of taxonomists: R. von Cosel from the Muséum National d"Histoire Naturelle de Paris (France); S. Gofas from the Department of animal biology of the Málaga University (Spain); C. Plum from the German Centre for Marine Biodiversity Research (Germany); M. Blazewicz-Paszkowycz from the University of Lodz (Poland); S. Vasilenko from the Russian Academy of Sciences of Moscow; A. Mironov, G.M. Vinogradov from the P.P. Shirshov Institute of Oceanology of Moscow; D. Ivanov from the Zoological Museum of the Moscow State University; N. Sanamyan from the Kamchatka Branch of the Pacific Institute of Geography of Petropavlovsk-Kamchatsky; E. Shornikov, M. Malyutina from the Institute of Marine Biology of Vladivostok (Russia); G. Vantsetti Murina from the Institute of Biology of the Southern Seas National Academy of Sciences of Ukraine. We also thank P. Pignet for her valuable help with ion analyses. The bathymetric maps were made with the data acquired and processed by B. Loubrieu (Ifremer). We also thank the anonymous reviewers for their comments that improved. The first version of the manuscript was professionally edited by C. Engel-Gautier. BR"s thesis, supervised by J.S. and D.D., was entirely funded by the French Institute for the Exploitation of the Sea (Ifremer). This research project benefited from funds from the HERMES and HERMIONE European projects (contract nos. 511234 and 226354) as well as from the ANR DEEP-OASES (ANR06BDV005) and support from the GDR ECCHIS.

References

Aloisi G, Bouloubassi I, Heijs SK, Pancost RD, Pierre C, Sinninghe Damste JS, Gottschal JC, Forney LJ, Rouchy JM (2002) CH_4-consuming microorganisms and the formation of carbonate crusts at cold seeps. Earth and Planetary Science Letters 203:195-203

Aloisi G, Pierre C, Rouchy JM, Foucher JP, Woodside J (2000) Methane-related authigenic carbonates of eastern Mediterranean Sea mud volcanoes and their possible relation to gas hydrate destabilisation. Earth and Planetary Science Letters 184:321-338

Barnes H, Blackstock J (1973) Estimation of lipids in marine animals and tissues: Detailed investigation of the sulphophosphovanilun method for 'total' lipids.

Journal of Experimental Marine Biology and Ecology 12:103-118
Barry JP, Kochevar RE, Baxter CH (1997) The influence of pore-water chemistry and physiology in the distribution of vesicomyid clam at cold seeps in Monterey Bay: Implications for patterns of chemosynthetic community organization. Limnology and Oceanography 42:318-328
Bellaiche G, Loncke L, Gaullier V, Mascle J, Courp T, Moreau A, Radan S, Sardou O (2001) The Nile Cone and its channel system: new results after the Fanil cruise. Comptes Rendus De L'Academie Des Sciences Série II Fascicule a-Sciences De La Terre Et Des Planètes 333:399-404
Bergquist DC, Urcuyo IA, Fisher CR (2002) Establishment and persistence of seep vestimentiferan aggregations on the upper Louisiana slope of the Gulf of Mexico. Marine Ecology Progress Series 241:89-98
Bright M, Giere O (2005) Microbial symbiosis in Annelida. Symbiosis 38:1-45
Brink RHJ, Dubach P, Lynch DL (1960) Measurement of carbohydrates in soil hydrolyzates with anthrone. Soil Science 89:157-166
Brissac T, Rodrigues CF, Gros O, Duperron S (2011) Characterization of bacterial symbioses in Myrtea sp. (Bivalvia: Lucinidae) and Thyasira sp. (Bivalvia: Thyasiridae) from a cold seep in the Eastern Mediterranean. Marine Ecology-An Evolutionary Perspective 32:198-210
Buscail R, Germain C (1997) Present-day organic matter sedimentation on the NW Mediterranean margin: Importance of off-shelf export. Limnology and Oceanogry 42:217-229
Camerlenghi A, Cita MB, Hieke W, Ricchiuto TS (1992) Geological evidence for mud diapirism on the Mediterranean Ridge accretionary complex. Earth and Planetary Science Letters 109:493-506
Campbell KA (2006) Hydrocarbon seep and hydrothermal vent paleoenvironments and paleontology: Past developments and future research directions. Paleogeography Paleoclimatology Paleoecology 232:362-407
Caprais JC, Lanteri N, Crassous P, Noël P, Bignon L, Rousseaux P, Pignet P, Khripounoff A (2010) CALMAR-A new submersible-operated benthic chamber: First application in the cold-seep environment of the Napoli mud volcano (Mediterranean Sea). Limnology And Oceanography: Methods 8: 304-312
Carlier A, Ritt B, Rodrigues C, Sarrazin J, Olu K, Grall J, Clavier J (2010) Heterogeneous energetic pathway and carbon sources for deep eastern Mediterranean cold-seep communities. Marine Biology 157:2545-2565
Cary SC, Vetter RD, Felbeck H (1989a) Habitat characterization and nutritional strategies of the endosymbiont-bearing bivalve *Lucinoma aequizonata.* Marine Ecology Progress Series 55:31-45
Cary C, Fry B, Felbeck H, Vetter RD (1989b) Multiple trophic resources for a chemoautotrophic community at a cold water brine seep at the base of the Florida Escarpment. Marine Biology 100:411-418
Cauwet G, Gadel F, Sierra MMD, Donard O, Ewald M (1990) Contribution of the Rhone river to rganic-carbon inputs to the northwestern Mediterranean Sea Continental Shelf Research 10:1025-1037
Charlou JL, Donval JP, Zitter T, Roy N, Jean-Baptiste P, Foucher JP, Woodside J (2003) Evidence of methane venting and geochemistry of brines on mud volcanoes of the eastern Mediterranean Sea. Deep Sea Research Part I: Oceanographic Research Papers 50:941-958
Cita MB, Ryan WBF (1973) Time scale and general synthesis, Washington, DC
Cita MB, Ryan WBF, Paggi L (1981) Prometheus mud breccia. An example of shale diapirism in the western Mediterranean Ridge. Annales Geologiques des Pays

Helleniques 13:37-49
Cita MB, Camerlenghi A (1990) The Mediterranean Ridge as an accretionary prism in collisional context. Memorie della Societa Geologica Italiana 45:463-480
Coleman DF, Ballard RD (2001) A highly concentrated region of cold hydrocarbon seeps in the southeastern Mediterranean Sea. Geo-Marine Letters 21:162-167
Cordes EE, Becker EL, Hourdez S, Fisher CR (2010) Influence of foundation species, depth, and location on diversity and community composition at Gulf of Mexico lower-slope cold seeps. Deep Sea Research Part II: Topical Studies in Oceanography 57:1870-1881
Corselli C, Basso D (1996) First evidence of benthic communities based on chemosynthesis on the Napoli mud volcano (eastern Mediterranean). Marine Geology 132:227-239
Dando PR, Southward AJ (1986) Chemoautotrophy in bivalve mollusks of the genus *Thyasira*. Journal of the Marine Biological Association of the United Kingdom 66:915-929
Dando PR, Southward AJ, Southward EC, Lamont P, Harvey R (2008) Interactions between sediment chemistry and frenulate pogonophores (Annelida) in the north-east Atlantic. Deep Sea Research Part I: Oceanographic Research Papers 55:966-996
Danovaro R, Marrale D, Della Croce N, Parodi P, Fabiano M (1999) Biochemical composition of sedimentary organic matter and bacterial distribution in the Aegean Sea: trophic state and pelagic-benthic coupling. Journal of Sea Research 42:117-129
Dubilier N, Bergin C, Lott C (2008) Symbiotic diversity in marine animals: the art of harnessing chemosynthesis. Nature Review Microbiology 6:725-740
Duperron S, Lorion J, Samadi S, Gros O, Gaill F (2009) Symbioses between deep-sea mussels (Mytilidae: Bathymodiolinea) and chemosynthetic bacteria: diversity, function and evolution. Comptes Rendus Biologies 332:298-310
Dupré S, Woodside J, Foucher JP, de Lange G, Mascle J, Boetius A, Mastalerz V, Stadnitskaia A, Ondreas H, Huguen C, Harmegnies FO, Gontharet S, Loncke L, Deville E, Niemann H, Omoregie E, Olu-Le RoyRoy K, Fiala-Medioni A, Dahlmann A, Caprais JC, Prinzhofer A, Sibuet M, Pierre C, Sinninghe Damste JS (2007) Seafloor geological studies above active gas chimneys off Egypt (Central Nile deep sea fan). Deep-Sea Research Part I-Oceanographic Research Papers 54:1146-1172
Feseker T, Foucher JP, Harmegnies F (2008) Fluid flow or mud eruptions? Sediment temperature distributions on Hakon Mosby mud volcano, SW Barents Sea slope. Marine Geology 247:194-207
Fichez R (1991) Composition and fate of organic-matter in submarine cave sediments - Implications for the biogeochemical cycle of organic carbon. Oceanologica Acta 14:369-377
Gauthier O, Sarrazin J, Desbruyeres D (2010) Measure and mis-measure of species diversity in deep-sea chemosynthetic communities. Marine Ecology Progress Series 402:285-302
Hessler RR, Jumars PA (1974) Abyssal community analysis from replicate box cores in the central North Pacific. Deep Sea Research 21:185-209
Hovland M, Gardner JV, Judd AG (2002) The significance of pockmarks to understanding fluid flow processes and geohazards. Geofluids 2:127-136
Hsu KJ, Montadert L, Bernoulli D, Cita MB, Erickson A, Garrison RE, Kidd RB, Melieres F, Muller C, Wright R (1977) History Of Mediterranean Salinity Crisis. Nature 267:399-403

Huguen C, Foucher JP, Mascle J, Ondreas H, Thouement M, Stadnitskaia A, Pierre C, Bayon G, Loncke L, Boetius A, Bouloubassi I, De Lange G, Caprais JC, Fouquet Y, Woodside J, Dupre S, and the NAUTINIL Scientific Party (2009) Menes Caldera, a highly active site of brine seepage in the Eastern Mediterranean Sea: "In situ" observations from the NAUTINIL expedition (2003) Marine Geology 261:138-152

Huguen C, Mascle J, Chaumillon E, Kopf A, Woodside J, Zitter T (2004) Structural setting and tectonic control of mud volcanoes from the Central Mediterranean Ridge (Eastern Mediterranean). Marine Geology 209:245-263

Huguen C, Mascle J, Woodside J, Zitter T, Foucher JP (2005) Mud volcanoes and mud domes of the Central Mediterranean Ridge: Near-bottom and in situ observations. Deep Sea Research Part I: Oceanographic Research Papers 52:1911

Ivanov MK, Limonov AF, vanWeering TCE (1996) Comparative characteristics of the Black Sea and Mediterranean Ridge mud volcanoes. Marine Geology 132:253-271

Jaccard P (1901) Distribution de la flore alpine dans le Bassin des Dranses et dans quelques régions voisines. Bulletin de la société vaudoise des sciences naturelles

Jackson DA (1995) PORTEST: a PROcustean randomization TEST of community environment concordance. Ecosciences 2:297-303

Jensen P (1992) 'An enteropneusts nest' - Results of the burrowing traits by the deep-sea acorn worm *Stereobalanus canadensis* (Spengel). Sarsia 77:125-129

Jerosch K, Schluter M, Foucher JP, Allais AG, Klages M, Edy C (2007) Spatial distribution of mud flows, chemoautotrophic communities, and biogeochemical habitats at Hakon Mosby Mud Volcano. Marine Geology 243:1-17

Judd AG, Hovland M (2007) Seabed Fluid Flow - The Impact on Geology, Biology and the Marine Environment, Cambridge University Press.

Julian D, Gaill F, Wood E, Arp AJ, Fisher CR (1999) Roots as a site of hydrogen sulfide uptake in the hydrocarbon seep vestimentiferan *Lamellibrachia* sp. Journal of Experimental Biology 202:2245-2257

Kaltin S, Haraldsson C, Anderson LG (2005) A rapid method for determination of total dissolved inorganic carbon in seawater with high accuracy and precision. Marine Chemistry 96:53-60

Kindt R, Coe R (2005) Tree diversity analysis. A manual and software for common statistical methods for ecological and biodiversity studies. World Agroforestry Centre (ICRAF), Nairobi

Koleff P, Gaston KJ, Lennon JJ (2003) Measuring beta diversity for presence–absence data. Journal of Animal Ecology 72:367-382

Krylova EM, Sahling H (2010) Vesicomyidae (Bivalvia): Current Taxonomy and Distribution. PLoS ONE 5:e9957

Kvenvolden KA, Rogers BW (2005) Gaia's breath - global methane exhalations. Marine And Petroleum Geology 22:579-590

Legendre P, Gallagher ED (2001) Ecologically meaningful transformations for ordination of species data. Oecologia 129:271-280

Levin LA (2005) Ecology of cold seep sediments: Interactions of fauna with flow, chemistry and microbes. In: Oceanography and marine biology - An annual review, Vol 43, Vol 43. Crc Press-Taylor & Francis Group, Boca Raton, p 1-46

Levin LA, Gage JD (1998) Relationships between oxygen, organic matter and the diversity of bathyal macrofauna. Deep Sea Research Part II: Topical Studies in Oceanography 45:129

Levin LA, Ziebis W, Mendoza GF, Growney VA, Tryon MD, Mahn C, Gieskes JM, Rathburn AE (2003) Spatial heterogeneity of macrofauna at northern California methane seeps: influence of sulfide concentration and fluid flow. Marine Ecology Progress Series 265:123-139

Levin LA, Mendoza GF, Gonzalez JP, Thurber AR, Cordes EE (2010) Diversity of bathyal macrofauna on the northeastern Pacific margin: the influence of methane seeps and oxygen minimum zones. Marine Ecology 31:94-110

Limonov AF, Woodside JM, Cita MB, Ivanov MK (1996) The Mediterranean Ridge and related mud diapirism: A background. Marine Geology 132:7-19

Loncke L, Mascle J, and the Fanil Scientific Party (2004) Mud volcanoes, gas chimneys, pockmarks and mounds in the Nile deep-sea fan (Eastern Mediterranean): geophysical evidences. Marine and Petroleum Geology 21:669-689

Lykousis V, Alexandri S, Woodside J, De Lange G, Dählmann A, Perissoratis C, Heeschen K, Ioakim C, Sakellariou D, Nomikou P, Rousakis G, Casas D, Ballas D, Ercilla G (2008) Mud volcanoes and gas hydrates in the Anaximander Mountains (Eastern Mediterranean Sea). Marine and Petroleum Geology 26:1-19

MacDonald IR, Reilly JF, Guinasso NL, Brooks JM, Carney RS, Bryant WA, Bright TJ (1990) Chemosynthetic mussels at a brine-filled pockmark in the Northern Gulf of Mexico. Science 248:1096-1099

MacDonald IR, Guinasso NL, Jr., Ackleson SG, Amos JF, Duckworth R, Sassen R, Brooks JM (1993) Natural Oil Slicks in the Gulf of Mexico Visible From Space. Journal of Geophysical Research 98:16351-16364

MacDonald IR, Buthman DB, Sager WW, Peccini MB, Guinasso NL, Jr. (2000) Pulsed oil discharge from a mud volcano. Geology 28:907-910

Mascle J, Sardou O, Loncke L, Migeon S, Camera L, Gaullier V (2006) Morphostructure of the Egyptian continental margin: Insights from swath bathymetry surveys. Marine Geophysical Researches 27:49-59

Mascle J, Zitter T, Bellaiche G, Droz L, Gaullier V, Loncke L (2001) The Nile deep sea fan: preliminary results from a swath bathymetry survey. Marine and Petroleum Geology 18:471-477

Menot L, Galéron J, Olu K, Caprais JC, Crassous P, Khripounoff A, Sibuet M (2010) Spatial heterogeneity of macrofaunal communities in and near a giant pockmark area in the deep Gulf of Guinea. Marine Ecology 31:78-93

Milkov AV (2000) Worldwide distribution of submarine mud volcanoes and associated gas hydrates. Marine Geology 167:29-42

Niemann H, Losekann T, de Beer D, Elvert M, Nadalig T, Knittel K, Amann R, Sauter EJ, Schluter M, Klages M, Foucher JP, Boetius A (2006) Novel microbial communities of the Haakon Mosby mud volcano and their role as a methane sink. Nature 443:854-858

Oksanen J, Blanchet FG, Kindt R, Legendre P, Minchin PR, O'Hara RB, Simpson GL, Solymos P, Henry MH, Stevens MHH, Wagner H (2012) vegan: Community Ecology Package - Ordination methods, diversity analysis and other functions for community and vegetation ecologist, http://cran.r-project.org/, http://vegan.r-forge.r-project.org/

Oliver G, Rodrigues C, Cunha MR Chemosymbiotic bivalves from the mud volcanoes of the Gulf of Cadiz. ZooKeys 113:1-38

Olu-Le Roy K, Caprais JC, Fifis A, Fabri MC, Galeron J, Budzinsky H, Le Menach K, Khripounoff A, Ondreas H, Sibuet M (2007) Cold-seep assemblages on a giant pockmark off West Africa: spatial patterns and environmental control. Marine Ecology-an Evolutionary Perspective 28:115-130

Olu-Le Roy K, Sibuet M, Fiala-Medioni A, Gofas S, Salas C, Mariotti A, Foucher J-P,

Woodside J (2004) Cold seep communities in the deep eastern Mediterranean Sea: composition, symbiosis and spatial distribution on mud volcanoes. Deep Sea Research Part I: Oceanographic Research Papers 51:1915-1936
Olu K, Lance S, Sibuet M, Henry P, Fiala-Medioni A, Dinet A (1997) Cold seep communities as indicators of fluid expulsion patterns through mud volcanoes seaward of the Barbados accretionary prism. Deep Sea Research Part I: Oceanographic Research Papers 44:811-819
Paull CK, Hecker B, Commeau R, Freeman-Lynde RP, Neumann C, Corso WP, Golubic S, Hook JE, Sikes E, Curray J (1984) Biological communities at the Florida Escarpment resemble hydrothermal vent taxa. Science 226:965-967
Peres-Neto PR, Jackson DA (2001) How well do multivariate data sets match? The advantages of a Procrustean superimposition approach over the Mantel test. Oecologia 129:169-178
Pierre C, Bayon G, Blanc-Valleron MM, Rouchy JM, Mascle A, Dupré S, Bouloubassi I, Sarrazin J, Foucher JP, and the Medeco scientific team (2008) Authigenic carbonate crusts from active cold seep sites in the Eastern Mediterranean. New results from the MEDECO cruise (HERMES Project). In: 9th International Conference on Gas in Marine Sediments, Bremen
Pierre C, Blanc-Valleron MM, Bouloubassi I, Cagatay MN, Foucher JP, Henry P, Mascle A, Zitter T (2010) Methane-related carbonates from cold seeps of eastern Medtierranean and Marmara sea. In. CIESM
R Development Core Team (2012). R: A language and environment for statistical computing. R Foundation for Statistical Computing, Vienna, Austria
Ritt B, Sarrazin J, Caprais JC, Noël P, Gauthier O, Pierre C, Henry P, Desbruyeres D (2010) First insights on the cold-seep benthic communities in the Marmara Sea. Deep-Sea Research I 57: 1120-1136
Ritt B, Pierre C, Gauthier O, Wenzhoefer F, Boetius A, Sarrazin J (2011) Diversity and distribution of cold-seep fauna associated with different geological and environmental settings at mud volcanoes and pockmarks of the Nile Deep-Sea Fan. Marine Biology 158:1187-1210
Ritt B, Duperron S, Lorion J, Lazar CS, Sarrazin J (2012) Integrative study of a new cold-seep mussel (Mollusca: bivalvia) associated with chemosynthetic symbionts in the Marmara Sea. Deep-Sea Research Part I: Oceanographic Research Papers 167:121-132
Rodrigues CF, Hilario A, Cunha MR, Weightman AJ, Webster G (2011) Microbial diversity in Frenulata (Siboglinidae, Polychaeta) species from mud volcanoes in the Gulf of Cadiz (NE Atlantic). Antonie Van Leeuwenhoek 100:83-98
Rouse GW, Pleijel F (2001) Polychaetes. Oxford University Press
Sahling H, Rickert D, Lee RW, Linke P, Suess E (2002) Macrofaunal community structure and sulfide flux at gas hydrate deposits from the Cascadia convergent margin, NE Pacific. Marine Ecology Progress Series 231:121-138
Salas C, Woodside J (2002) *Lucinoma kazani* n. sp. (Mollusca: Bivalvia): evidence of a living benthic community associated with a cold seep in the Eastern Mediterranean Sea. Deep Sea Research Part I: Oceanographic Research Papers 49:991-1005
Sarradin PM, Caprais JC (1996) Analysis of dissolved gases by headspace sampling gas chromatography with column and detector switching. Preliminary results. Analytical Communications 33:371-373
Sibuet M, Olu K (1998) Biogeography, biodiversity and fluid dependence of deep-sea cold-seep communities at active and passive margins. Deep Sea Research Part II: Topical Studies in Oceanography 45:517-567

Sibuet M, Olu-Le Roy K (2002) Cold Seep communities on continental margins: Structure and quantitative distribution relative to geological and fluid venting patterns. In: G. Wefer DB, D. Hebbeln, B.B. Jorgensen, T. Van Weering (ed) Ocean Margin Systems. Springer Verlag, Berlin, p 235-251

Southward EC, Andersen AC, Hourdez S (2011) *Lamellibrachia anaximandri* n. sp., a new vestimentifera tubeworm from the Mediterranean (Annelida). Zoosystema 33: 245-279

Stevenson FJ, Cheng CN (1970) Amino acids in sediments: Recovery by acid hydrolysis and quantitative estimation by a colorimetric procedure. Geochimica et Cosmochimica Acta 34:77-88

Thistle D (2003) The deep-sea floor: an overview. In: Ecosystems Of The Deep Ocean, Vol 28. Elsevier Science Bv, p 5-37

Van Gaever S, Moodley L, de Beer D, Vanreusel A (2006) Meiobenthos at the Arctic Hakon Mosby Mud Volcano, with a parental-caring nematode thriving in sulphide-rich sediments. Marine Ecology Progress Series 321:143-155

Vuillemin R, Le Roux D, Dorval P, Bucas K, Sudreau JP, Hamon M, Le Gall C, Sarradin PM (2009) CHEMINI: A new in situ CHEmical MINIaturized analyzer. Deep Sea Research Part I: Oceanographic Research Papers 56:1391-1399

Werne JP, Haese RR, Zitter T, Aloisi G, Bouloubassi I, Heijs S, Fiala-Medioni A, Pancost RD, Sinninghe Damste JS, de Lange G (2004) Life at cold seeps: a synthesis of biogeochemical and ecological data from Kazan mud volcano, eastern Mediterranean Sea. Chemical Geology 205:367-390

Winkler LW (1888) Die Bestimmund des im Wasser gelosten Sauerstoffes. Ber Dtsch Chem Ges 27:2843-2855

Woodside JM, Ivanov MK, Limonov AF, Expeditions SSotA (1998) Shallow gas and gas hydrates in the Anaximander Mountains regions, eastern Mediterranean Sea. In: Henriet J-P, and Mienert, J. (ed) Gas Hydrates: Relevance to World Margin Stability and Climate Change. Geological Society, London, p 177-193

Woodside JM, Mascle J, Zitter TAC, Limonov AF, Ergun M, Volkonskaia A (2002) The Florence Rise, the Western Bend of the Cyprus Arc. Marine Geology 185:177-194

Zitter T (2004) Mud volcanism and fluid emissions in Eastern Mediterranean neotectonic zones. Free University of Amsterdam - Faculty of Earth and Life Science

Zitter TAC, Huguen C, Woodside JM (2005) Geology of mud volcanoes in the eastern Mediterranean from combined sidescan sonar and submersible surveys. Deep-Sea Research Part I-Oceanographic Research Papers 52:457-475

Zitter TAC, Woodside JM, Mascle J (2003) The Anaximander Mountains: a clue to the tectonics of southwest Anatolia. Geological Journal 38:375-394

Abbreviation list

Bio-av. OM: Bio-available organic matter
Biv: Bivalve microhabitat
CarbH: Total carbohydrates
CC: Carbonate crust microhabitat
Co: Concretions
DIC: Dissolved inorganic carbon
ES50: Expected richness for a sample of 50 individuals
Lam: *Lamellibrachia* microhabitat

MR: Mediterranean Ridge
MV: Mud volcano
NDSF: Nile Deep-Sea Fan
OM: Organic matter
PCA: Principal component analysis
Pcc: Periphery of the Carbonate crust microhabitat
Plam: Periphery of the *Lamellibrachia* microhabitat
RDA: Redundancy analysis
Red: Reduced sediment microhabitat
Ref: Reference site
ROV: Remotely operated vehicle
RTS: Right tail-sum intrinsic diversity profiles
SBF: Symbiont-bearing fauna
Sed: Sediments
S_{obs}: Observed taxonomic richness
TC: Total carbon
THAA: Total hydrolysable amino acids
TN: Total nitrogen
TOC: Total organic carbon
ww: Wet weight

Tables

Table 1. : Sample location, depth and gear used to perform physico-chemical and faunal sampling on different microhabitats from the Napoli and Amsterdam (MVs) in the eastern Mediterranean Sea explored during the MEDECO cruise (2007). Sampling effort, length of each sediment core and estimated surface of each carbonate crust are also reported. ΣS = (H_2S+HS^-+S^{2-}), OC: Organic Carbon, TN: Total Nitrogen, OM: Organic Matter.

Microhabitat types	Latitude (°N)	Longitude (°E)	Depth (m)	Physico-chemical sampling		Faunal sampling
				Sediment-water interface	Porewater in sediments	
Olimpi mud field – Napoli MV						
Bivalve shells (Biv)	33°43.75"	24°40.95"	1942	3 measures of ΣS with CHEMINI 3x2 water samples with PEPITO: CH_4 , pH, O_2, SO_4^{2-} , Cl^-	3x2 push corers: O_2, SO_4^{2-} , Cl^- profiles % OC, TN, total lipids, total amino acids, total carbohydrates, % bio-available OM and % carbonates	3 blade corers (200 cm²) Biv1 (21 cm) Biv2 (15 cm) Biv3 (21 cm)
Lamellibrachia (Lam)	33°43.75"	24°40.94"	1942	3 measures of ΣS with CHEMINI 3x2 water samples with PEPITO: CH_4 , pH, O_2, SO_4^{2-} , Cl^- 1 CALMAR	3x2 push corers: O_2, SO_4^{2-} , Cl^- profiles % OC, TN, total lipids, total amino acids, total carbohydrates, % bio-available OM and % carbonates	3 blade corers (200 cm²) Lam1 (12 cm) Lam2 (16 cm) Lam3 (12 cm)
Carbonate crusts (CC)	33°43.78"	24°40.95"	1941	3 measures of ΣS with CHEMINI 3x2 water samples with	None	3 suction samplers 3 pieces of crust CC1 (425 cm²)

				PEPITO: CH_4 , pH, O_2, SO_4^{2-} , Cl^-		CC2 (641 cm²) CC3 (277 cm²)
Lam Periphery 2m away (Plam-A)	33°43.75"	24°40.94"	1943	2 water samples with PEPITO: CH_4 , pH, O_2, SO_4^{2-} , Cl^-	2 push corers: O_2, SO_4^{2-} , Cl^- profiles % OC[a]	2 blade corers (200 cm²) Plam1 (15 cm) Plam2 (15 cm)
Lam Periphery 5m away (Plam-B)	33°43.75"	24°40.94"	1942	2 water samples with PEPITO: CH_4 , pH, O_2, SO_4^{2-} , Cl^-	2 push corers: O_2, SO_4^{2-} , Cl^- profiles % OC[a]	2 blade corers (200 cm²) Plam3 (10 cm) Plam4 (11 cm)
CC Periphery 6m away (Pcc-A)	33°43.78"	24°40.95"	1941	2 water samples with PEPITO: CH_4 , pH, O_2, SO_4^{2-} , Cl^-	2 push corers: O_2, SO_4^{2-} , Cl^- profiles % OC[a]	2 blade corers (200 cm²) Pcc1 (10 cm) Pcc2 (17 cm)
CC Periphery 22m away (Pcc-B)	33°43.77"	24°40.93"	1941	2 water samples with PEPITO: CH_4 , pH, O_2, SO_4^{2-} , Cl^-	2 push corers: O_2, SO_4^{2-} , Cl^- profiles % OC[a]	2 blade corers (200 cm²) Pcc3 (15 cm) Pcc4 (11 cm)
Reference site (Ref)	33°43.31"	24°38.60"	2010	None	% OC, TN, % carbonate	1 box core (0.25 m², 10 cm)
Anaximander Mountains – Amsterdam MV						
Bivalve shells (Biv)	35°20.08"	30°16.12"	2024	3x2 water samples with PEPITO: CH_4 , pH, O_2, SO_4^{2-} , Cl^-	1 push corer [b]: % OC, TN, total lipids, total amino acids, total carbohydrates, % bio-available OM and % carbonates	2 blade corers (200 cm²) Biv1 (19 cm) Biv2 (14 cm)
Reduced sediments (Red)	35°20.10"	30°16.09"	2023	2x2 water samples with PEPITO: CH_4 , pH, O_2, SO_4^{2-} , Cl^-	No exploitable push corer	4 blade corers (200 cm²) Red1 (15 cm) Red2 (13 cm) Red3 (15 cm) Red4 (12 cm)
Carbonate crusts (CC)	35°20.08"	30°16.30"	2025	2 water samples with PEPITO: CH_4 , pH, O_2, SO_4^{2-} , Cl^-	No exploitable push corer	1 suction sampler 3 pieces of crust CC1 (162 cm²) CC2 (162 cm²) CC3 (125 cm²)
Reference site (Ref)	35°20.99"	30°18.00"	2152	None	% OC, TN, % carbonate	1 box core (0.25 m², 10 cm)

[a] %OC performed independently to the organic matter characterisation

[b] because of the presence of clasts in the push cores, only one could be used for chemical analyses

Table 2. Chemical characteristics of microhabitats on each mud volcano. Visual observations of sediment colour at each microhabitat as well as pH measurements, dissolved oxygen, methane (mean ± SD, no. of replicates in parentheses), sulphate, and chloride concentrations at the sediment-water interface in the replicates of each microhabitat sampled at the Napoli and Amsterdam mud volcanoes during the MEDECO cruise (2007). The highest values at each mud volcanoes are highlighted in bold. Microhabitat codes as in Table1; -: not measured

	Visual observations	pH	$[O_2]$ (µmol l^{-1})	$[CH_4]$ (µmol l^{-1})	$[SO_4^{2-}]$ (mmol l^{-1})	$[Cl^-]$ (mmol l^{-1})
Napoli mud volcano						
Biv1	Brown sediments	**8.03**	212.6	0.29 ± 0.00 (3)	30.0	571 [a]
Biv2		-	199.1	0.51 ± 0.03 (3)	29.5 [a]	582 [a]
Biv3		8.00	215.8	0.44 ± 0.02 (3)	30.8	585
Lam1	Black sediments with sulphide smell	8.02	**222.5**	0.35 ± 0.05 (6)	**31.0**	588
Lam2		8.02	205.8	0.36 ± 0.05 (5)	30.9	586
Lam3		7.99	212.0 [a]	0.76 ± 0.12 (4)	30.8	584
CC1	Dark crusts with cemented fragments of bivalve shells and tubes	8.00	196.4	**4.29 ± 2.19** (5)	30.8[a]	587
CC2		8.01	199.4	2.87 ± 1.22 (5)	**31.0**	**591**
CC3		**8.03**	196.9	2.27 ± 0.09 (7)	30.8	585
Plam-A	Brown sediments	8.01	207.3	0.35 ± 0.06 (5)	30.9	585
Plam-B		8.02	221.4	0.56 ± 0.02 (2)	30.9	584
Pcc-A	Brown sediments	8.02	210.7	0.46 ± 0.06 (6)	**31.0**	589
Pcc-B		8.02	199.5	0.50 ± 0.04 (9)	30.9	587
Amsterdam mud volcano						
Biv1	Brown sediments	8.02	195.5	0.70 ± 0.02 (5)	30.7	586
Biv2		8.02	186.8	0.41 ± 0.05 (6)	**30.8**	587
Red1/Red2	Black sediments with sulphide smell and gas bubbles	8.03 [b]	188.2 [b]	**12.45 ± 2.10** [b] (5)	27.6 [b]	530 [b]
Red3/Red4		**8.08** [b]	191.7 [b]	2.37 ± 0.16 [b] (6)	30.7 [b]	585 [b]
CC1	Grey crusts with cemented fragments of bivalve shells	8.02	194.2	0.60 ± 0.04 (3)	30.6	583
CC2		8.03	198.2	0.56 ± 0.02 (2)	**30.8**	**588**
CC3		8.02	**202.2**	0.25 ± 0.12 (2)	30.6	581

[a] O_2, SO_4^{2-}, Cl^- concentrations measured in supernatant water at the top of push corers instead of PEPITO sampling

[b] Unique values assessed from the unique water sample taken between Red1 and Red2, and between Red3 and Red4

Table 3. Percentage of organic carbon and composition of organic matter in surface sediments of the different microhabitats from Napoli and Amsterdam mud volcanoes: total nitrogen (TN), C:N molar ratio, total lipids (Lipids), total carbohydrates (CarbH), total hydrolysable amino acids (THAA), proportion of bio-available organic matter (bio-av. OM) and percentages of carbonates; -: not measured; DW: dry weight. Microhabitat codes as in Table 1.

Micro-habitat	Organic C (% DW)	TN (% DW)	C:N (molar)	Lipids (mg g^{-1})	CarbH (mg g^{-1})	THAA (mg g^{-1})	Bio-av. OM (% total OM)	Carbonate (% DW)
Napoli mud volcano								
Biv1	0.27 [a]	-	-	-	-	-	-	-
Biv2	0.53 [b]	0.054	11.3	0.171	1.253	0.821	23.7	29.1
Lam1	1.82 [b]	0.247	8.6	0.900	3.006	8.440	37.7	-
Lam2	1.67 [b]	0.218	9.0	0.846	3.288	8.169	40.8	24.5
Lam3	1.70 [b]	0.180	11.0	0.891	3.011	8.731	41.4	-
Plam-A	0.41 [a]	-	-	-	-	-	-	-
Plam-B	0.82 [a]	-	-	-	-	-	-	-
Pcc-A	0.67 [a]	-	-	-	-	-	-	-
PCc-B	0.47 [a]	-	-	-	-	-	-	-
Ref	0.57 [b]	0.038	17.5	-	-	-	-	47
Amsterdam mud volcano								
Biv1	0.60 [b]	0.055	12.7	0.219	0.846	1.848	26.9	23.3
Ref	0.62 [b]	0.066	11.0	-	-	-	-	39

[a] Auto-analyser (LECO WR 12) after sediment decarbonation with 6 N HCL
[b] Automatic CN-analyser (LECO 2000) after acidification with 2 N HCL

Table 4. Macrofaunal (>250 µm) relative abundances (%) of each taxa in the active microhabitats studied on the Napoli mud volcano: sediments with bivalve shells (Biv, n = 3), *Lamellibrachia* (Lam, n = 3), carbonate crusts (CC, n = 3), sediments from the periphery of the *Lamellibrachia* microhabitat (Plam, n = 4), sediments from the periphery of the carbonate crust microhabitat (Pcc, n = 4) and reference site (Ref, n = 1) and on the Amsterdam mud volcano: sediments with bivalve shells (Biv, n = 2), reduced sediments (Red, n = 4), carbonate crusts (CC, n = 3) and reference (Ref, n = 1). Total relative abundance for each taxonomic group are highlighted in **bold**. *: taxonomic level used for α-diversity analyses (mostly family-level); **: taxonomic level used for α -diversity for Plam and Ref only; juv.= juvenile, und.= undetermined. All samples were taken during the MEDECO cruise (2007).

	Napoli						Amsterdam			
Taxonomic groups	**Biv**	**Lam**	**CC**	**Plam**	**Pcc**	**Ref**	**Biv**	**Red**	**CC**	**Ref**
Porifera (Total)	**8.39**	**0**	**27.03**	**0**	**0**	**0**	**0**	**0**	**0**	**0**
Demospongia*	6.99	0	18.38	0	0	0	0	0	0	0
Hexactinellida*	1.40	0	8.65	0	0	0	0	0	0	0
Cnidaria (Total)	**20.28**	**0.89**	**13.51**	**0.43**	**0**	**3.85**	**0**	**0**	**0**	**0**
Anthozoa – Zoantharia										
Parazoanthidae*										
Isozoanthus sp.1	0	0	5.41	0	0	0	0	0	0	0
Anthozoa - Actiniaria										
Sargatiidae*										
Sagartiogeton sp.	0	0.45	0.54	0	0	0	0	0	0	0
Und. Sargatiidae	3.50	0	0	0	0	0	0	0	0	0
Und. Actiniaria*	0	0	0	0.43	0	0	0	0	0	0
Medusozoa – Scyphozoa										
Und. Scyphozoa*	16.78	0.45	7.57	0	0	3.85	0	0	0	0
Polychaeta (Total)	**49.65**	**47.32**	**24.86**	**44.02**	**15.91**	**61.54**	**51.82**	**38.21**	**80.70**	**67.24**
Capitellidae*	0	0	2.70	1.71	0	7.69	5.26	0.05	0	13.79
Chrysopetalidae*	0	0	0	0	0	0	0	0	0	34.48
Cirratulidae*	1.40	0	0	15.81	0.94	7.69	16.60	0	8.77	0
Dorvilleidae*	0.70	1.34	0.54	0.43	0.47	0	4.05	23.53	0	0
Flabelligeridae*	0	0	0	0	0	0	0	0	0	1.72
Glyceridae*	0	0	0	0.85	0	3.85	0.40	0	0	0
Hesionidae*	0.70	7.14	0.54	0	0	0	0	0	0	3.45
Lumbrineridae*	0	0	0	0	0.35	0	0.81	0	0	0
Opheliidae*	0	0	0	0	0	0	0	0	0	5.17
Orbiniidae*	1.40	0	0	0	0	7.69	0	0	0	0
Paraonidae*	24.48	0	0	17.09	11.00	0	22.27	0.05	12.28	1.72
Phyllodocidae*	0	5.36	2.70	0.43	0	0	0.81	0	0	0
Pilargidae*	0.70	0	1.62	0	0	0	0	0	0	0
Sabellidae*	0	0	0	0	0	0	0	0	0	1.72
Scalibregmatidae*	0	0	0	0	0	3.85	0	0	0	0
Serpulidae*	0	0	8.11	0	0	0	0	0	52.63	0
Siboglinidae-Frenulata*										
Siboglinum sp.	11.89	0	0	0.85	0.23	0	0.40	0	1.75	0
Siboglinidae-Obturata*										
Lamellibrachia anaximandri	0	25.00	1.08	0	0	0	0	0	0	0
Spionidae*	1.40	1.79	2.70	0.43	2.69	19.23	1.21	4.66	5.26.	0
Syllidae*	0.70	0	0	0	0	0	0	0	0	0
Terebellida*	6.29	6.70	4.32	6.41	0.23	3.85	0	9.92	0	5.17
Und. Larvae	0	0	0.54	0	0	0	0	0	0	0
Und. Polychaeta	0	0	0	0	0	7.69	0	0	0	0
Bivalvia (Total)	**0.70**	**0.89**	**2.70**	**18.38**	**2.92**	**0**	**9.31**	**61.29**	**3.51**	**0**
Lucinidae*										
Myrtea amorpha	0	0	0	2.56	0	0	0	0	0	0
Lucinoma kazani	0	0	0	0	0	0	0.40	0	0	0
Und. Lucinidae	0	0	0	1.28	0					
Thyasiridae*										
Thyasiria striata	0	0	0	0	0.58	1.62	0.15	1.75	1.75	0
Axinulus croulinensis	0	0	0	3.85	0.12	0	0	0	0	0

Und. Thyasiridae	0	0	0	8.55	0.58	0	0	0	0	0
Vesicomyidae*										
Isorropodon perplexum	0	0	0	0	0	0	0	0.05	0	0
Und. Vesicomyidae	0	0	0	0	0	0	4.86	61.03	1.75	0
Mytilidae*										
Idas aff. *modiolaeformis*	0.70	0.89	1.08	0	0	0	0	0	0	0
Und. Bivalvia	0	0	1.62	2.14	1.64	0	2.43	0.05	0	0
Gastropoda (Total)	**11.19**	**5.36**	**22.70**	**0.43**	**0**	**0**	**0.40**	**0**	**12.28**	**24.14**
Calliotropidae*										
Putzeysia wiseri	1.40	0	3.24	0	0	0	0	0	0	0
Orbitestellidae*										
Lurifax vitreus	4.90	0	12.43	0	0	0	0.40	0	10.53	0
Skeneidae*										
Und. Skeneidae	0	3.57	0	0	0	0	0	0	0	0
Conidae*										
Taranis moerchi	0.70	0	1.62	0	0	0	0	0	0	0
Cocculinidae*										
Coccopigya sp.	0	0	0.54	0	0	0	0	0	0	0
Cuspidariidae*										
Cuspidaria sp.	1.40	0	0	0	0	0	0	0	0	0
Und. Gastropoda**	2.80	1.79	4.86	0.43**	0	0	0	0	1.75	24.14**
Aplacophora (Total)	**0**	**0**	**0**	**0.85**	**0.12**	**7.69**	**2.83**	**0**	**0**	**0**
Chaetodermatidae*										
Falcidens gutturosus	0	0	0	0.85	0.12	7.69	2.83	0	0	0
Polyplacophora (Total)	0	0	0	0	0	0	0	0	0	3.45
Und. Polyplacophora*	0	0	0	0	0	0	0	0	0	3.45
Sipuncula (Total)	**1.40**	**0**	**2.16**	**0.85**	**0**	**11.54**	**0.40**	**0**	**0**	**0**
Phascolosomatidae*										
Apionsoma murina	1.40	0	0	0.85	0	0				
Phascolosoma aff. *granulatum*	0	0	0	0	0	0	0.40	0	0	0
Golfingiidae*										
Nephasoma sp. juv.	0	0	0.54	0	0	0	0	0	0	0
Nephasoma liljeborgi	0	0	1.62	0	0	0	0	0	0	0
Und. Sipuncula*	0	0	0	0	0	11.54	0	0	0	0
Echiuria (Total)	**0.70**	**0**	**0**	**0**	**0**	**0**	**0**	**0**	**0**	**0**
Echiuridae*										
Echiurus abyssalis	0.70	0	0	0	0	0	0	0	0	0
Nemerta (Total)	**0**	**0**	**0**	**0**	**0**	**7.69**	**0**	**0**	**0**	**3.45**
Und. Nemerta*	0	0	0	0	0	7.69	0	0	0	3.45
Crustacea (Total)	**7.69**	**45.54**	**7.03**	**35.04**	**81.05**	**7.69**	**35.22**	**0.51**	**3.51**	**0**
Amphipoda-Gammaridae										
Sebidae*										
Seba sp.	0	0	1.62	0	0	0	0	0	0	0
Lysianasidae*										
Orchomene grimaldii	0	5.80	0	0	0	0	0	0	0	0
Calliopiidae*										
Bouvierella carcinophila	0	23.66	0	0.85	0.23	0	0	0	0	0
Oedicerotidae*										
Monoculodes sp.	0	0	0	1.28	0.12	0	1.21	0	0	0
Oedicerotidae gen. sp.	0	0	0	0.43	0	0				
Periculodes aff. *longimanus*	0	0	0	0.85	0	0	0	0.25	0	0
Phoxocephalidae*										
Harpiniopsis sp.	0	0	0	0	0	0	0.40	0	1.75	0
Stegocephalidae*										
Stegocephaloides christianiensis	0	0	1.62	0	0	0	0	0	0	0
Und. Gammaridae	0	6.70	0	0	0	0	0.40	0	0	0
Cumacea										
Diastyloidae*										
Diastyloides serrata	2.80	0	0	6.84	0	0	0	0	0	0
Diastylis sp.	0	0	0	0	0.35	0	0	0.15	0	0
Isopoda-Asellota										
Munnopsidae*										
Disconectes sp.1	0.70	0	0	0	0.12	0	2.02	0	0	0
Disconectes sp.2	0.70	0	0	0	0	0	0	0	0	0
Ilyarachna sp.1	0	0	0	0	0.23	0	1.62	0	0	0

Ilyarachna sp.2	0	0	0	0	0	0	0	0.05	0	0
Ilyarachna sp.juv.	0	0	0	0	0.12	0	0	0	0	0
Unid. *Ilyarachna* sp.	0	0	0	0	0.12	0	0	0	0	0
Desmosomatidae*										
Chelator sp.	0	0	1.62	0	7.37	0	0	0	0	0
Eugerda sp.1	0	0	0.54	10.26	4.68	0	1.21	0	0	0
Eugerda sp.2	0	0	0	2.99	1.05	0	4.45	0	0	0
Eugerda sp.3	0	0	0	0	0.12	0	0	0	0	0
Eugerda filipes	0	0	0	0.43	0.12	0	0	0	0	0
Unid. *Eugerda* sp.	0	0	0	0.43	0.23	0	0	0	0	0
Eugerda sp. juv.	0	0	0	0	0	0	0.40	0	0	0
Pseudogerda atypicum	0	0	0	0	0	0	1.62	0	0	0
Whoia sp.	0	0	0	0	0.12	0	0	0	0	0
Desmosoma aff. *tyrrhencium*	0	0	0	2.99	0	0	0	0	0	0
Desmosoma aff. *elegans*	0	0	0	0	0.35	0	0	0	0	0
Desmosoma elegans	0	0	0	1.28	0	0	0	0	0	0
Desmosomatidae juv.	0	0	0	0	0.12	0	0	0	0	0
Und. Desmosomatidae	0	0	0.54	0	0	0	0	0	0	0
Isopoda-Epicaridae										
Und. Epicaridae*	0	0.45	0	0	0	0	0	0	0	0
Und. Isopoda	0	0	0	0	0	0	1.21	0	0	0
Leptostraca										
Und. Leptostraca*	0	8.93	0	0	0	0	0	0	0	0
Tanaidacea										
Pseudotanaidae*										
Pseudotanais sp.	0	0	0	3.85	0.12	0	0.40	0	0	0
Agathotanaidae*	0	0	0	1.28	65.49	0	18.22	0	0	0
Anarthruridae*	0	0	0	0.43	0	0	0	0	0	0
Paragnathotanaidae*	0.70	0	0	0.85	0	0	0.40	0	0	0
Leptognathiellidae*										
Leptognathiellidae sp.1	2.10	0	1.08	0	0	0	0.81	0	0	0
Leptognathiellidae sp.2	0.70	0	0	0	0	0	0	0	1.75	0
Tanallidae*										
Tanaella sp.	0	0	0	0	0	0	0.40	0	0	0
Und. Tanaidacea**	0	0	0	0	0	7.69**	0.40	0	0	0
Decapoda										
Und. Decapoda*	0	0	0	0	0	0	0	0.05	0	0
Echinodermata (Total)	**0**	**0**	**0**	**0**	**0**	**0**	**0**	**0**	**0**	**1.72**
Und. Echinoida*	0	0	0	0	0	0	0	0	0	1.72
Total abundance (number of individuals)	**143**	**224**	**185**	**234**	**855**	**26**	**247**	**1976**	**57**	**58**

Table 5. Biological descriptors of the studied microhabitats for the NAPOLI mud volcano sampled in the Mediterranean Sea. The observed taxonomic richness is given at the family level. The *number equivalents* of the Shannon and Simpson indices are given in italics. The highest values are highlighted in bold. n = 3 for all microhabitats + periphery, except for the reference site where n = 1. ES50: expected richness for a sample of 50 individuals; S_{obs}: observed taxonomic richness; -: not measured. Microhabitat codes as in Table 1

Biological descriptors	**Bivalve shells**	***Lamellibrachia***	**Carbonate crusts**	**Periphery (Plam, Pcc)**	**Reference site**
Mean macrofaunal densities (ind. m^{-2})	2 383 ± 289	3 733 ± 3 523	1 619 ±1 147	Plam: 2 925 ± 1 577 **Pcc: 10 688 ± 12 825**	104
Mean Jaccard"s similarity	**0.39**	0.36	0.38	Plam:0.33 / Pcc:0.27	-
Symbiont-bearing fauna	7.8 – 17.7%	**14.2 – 75.0%**	0 – 3.7%	Plam: 1 – 6.3% Pcc: 0 – 3.5%	0%
Total biomass (kg preserved wet weight m^{-2})	0.0033 ± 0.004	**4.73 ± 1.05**	0.019 ± 0.03	Plam: 0.0005 ± 0.0007 Pcc: 0.00032 ± 0.0003	-
Richness (S_{obs})	**25**	14	24	Plam:22 / Pcc:17	12
ES50	16	10	**17**	Plam:13 / Pcc:6	12
Shannon (H_e')	2.52	2.11	**2.70**	Plam:2.40 / Pcc:1.18	2.36
Exp (H_e')	*12.43*	*7.77*	***14.88***	*11.02 / 3.25*	*10.59*
Simpson (D_{GS})	0.87	0.83	**0.91**	Plam:0.88 / Pcc:0.53	0.89
1 / (1-D_{GS})	*7.99*	*5.81*	***10.65***	*8.24 / 2.11*	*9.29*
Evenness (*J'*)	0.78	0.78	0.85	Plam:0.78 / Pcc:0.42	**0.95**

Table 6.
Biological descriptors of the studied microhabitats for the AMSTERDAM mud volcano sampled in the Mediterranean Sea. The observed taxonomic richness is given at the family level. The *number equivalents* of the Shannon and Simpson indices are given in italics. Only the large meiofauna >250 µm was considered in this study. The higher values are highlighted in bold. n = 2 for the bivalve shell microhabitat, n = 4 for the reduced sediments, n = 3 for the carbonate crusts and n=1 for the reference site. ES50: expected richness for a sample of 50 individuals; S_{obs}: observed taxonomic richness; -: not measured. Microhabitat codes as in Table 1

Biological descriptors	**Bivalve shells**	**Reduced sediments**	**Carbonate crusts**	**Reference site**
Mean macrofaunal densities (ind. m^{-2})	6 175 ± 3 712	**24 700 ± 7 477**	1 222 ± 727	232
Mean Jaccard"s similarity	0.43	**0.55**	0.48	-
Symbiont-bearing fauna	2.8 – 9.0%	**41.7 – 77.2%**	0 – 9.1%	0%
Total biomass (kg preserved wet weight m^{-2})	0.021 ± 0.02	**0.049 ± 0.02**	0.0012 ± 0.002	-
Richness (S_{obs})	**25**	11	10	12
ES50	**13**	4	9	11
Shannon (H_e')	**2.36**	1.06	1.57	1.92
Exp (H_e')	**10.70**	*2.89*	*4.81*	*6.82*
Simpson (D_{GS})	**0.86**	0.56	0.67	0.79
1 / (1-D_{GS})	***7.28***	*2.27*	*3.06*	*4.85*
Evenness (*J'*)	0.73	0.44	0.68	**0.77**

Figures

Figure 1. (a) Eastern Mediterranean Sea with the localisation of the sampling sites and the position of the Mediterranean Ridge (black lines). Bathymetric maps of the remotely operated vehicles dives, localisation of the microhabitats and the reference sites on (b, c) the Napoli mud volcano (MV), located in the Olimpi field at 33°43.75'N, 24°40.95'E and (d, e) the Amsterdam MV, located in the Anaximander Mountains at 35°20.10'N, 30°16.09'E. Both MVs were sampled during the MEDECO cruise (Leg 1) in 2007.

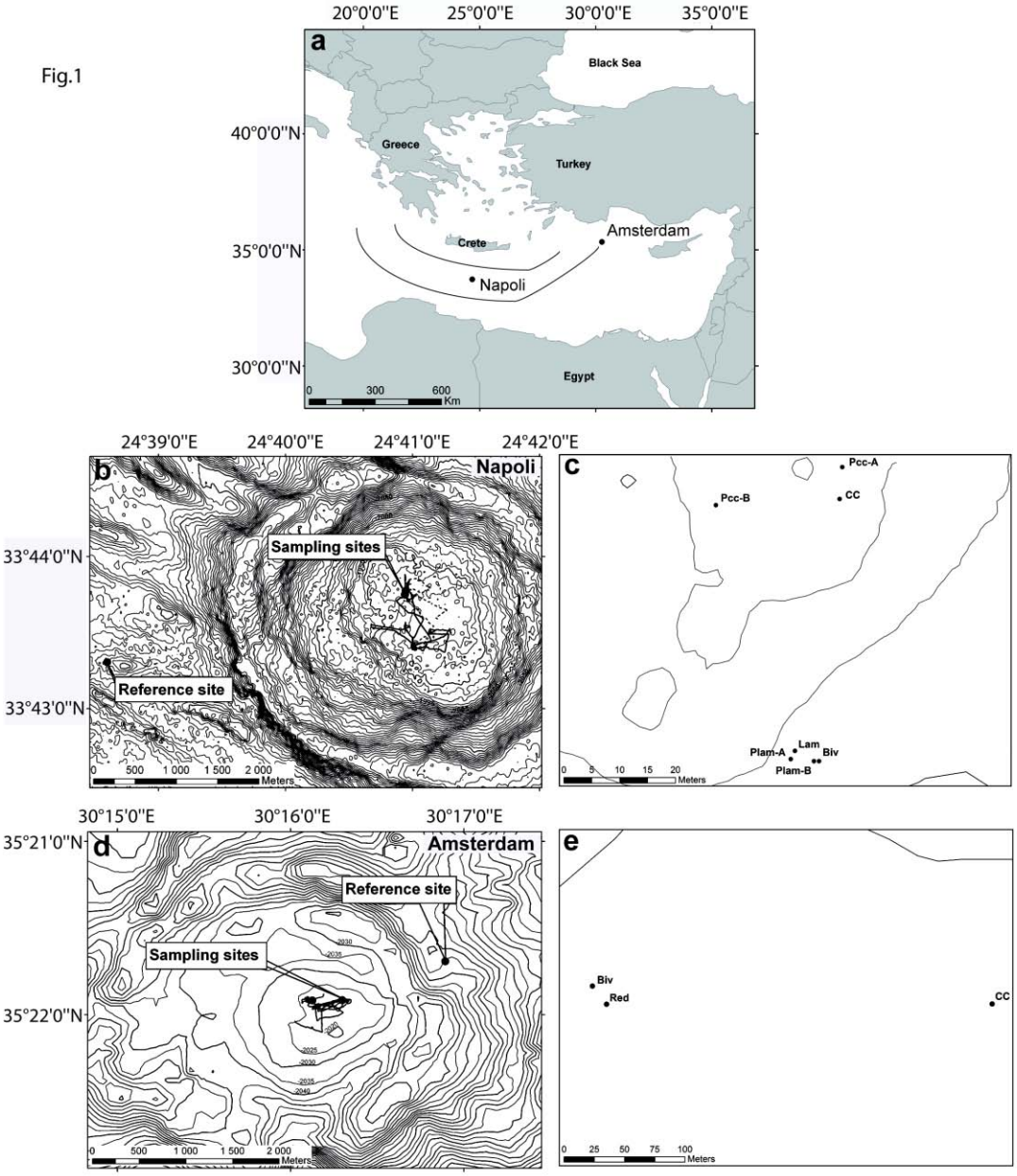


Figure 2. Typical photographs of the microhabitats sampled on Napoli (a-e) and Amsterdam (g-i) mud volcanoes (MVs): bivalve shells (a, Biv), *Lamellibrachia* (b, Lam), carbonate crusts (c, CC), brown sediments from the *Lamellibrachia* periphery (d, Plam), and the carbonate crust periphery (e, Pcc) on the Napoli MV. Bivalve shells (g, Biv), reduced sediments (h, Red) and carbonate crusts (i, CC) on the Amsterdam MV. The CALMAR benthic chamber (f) was deployed above one *Lamellibrachia* patch on Napoli. Blade corers were used to sample fauna in soft sediments (a, d, e, g, h) while the ROV suction sampler was used to sample the epifauna on the carbonate crusts (i). All microhabitats were sampled during the MEDECO cruise (2007).

Fig.2

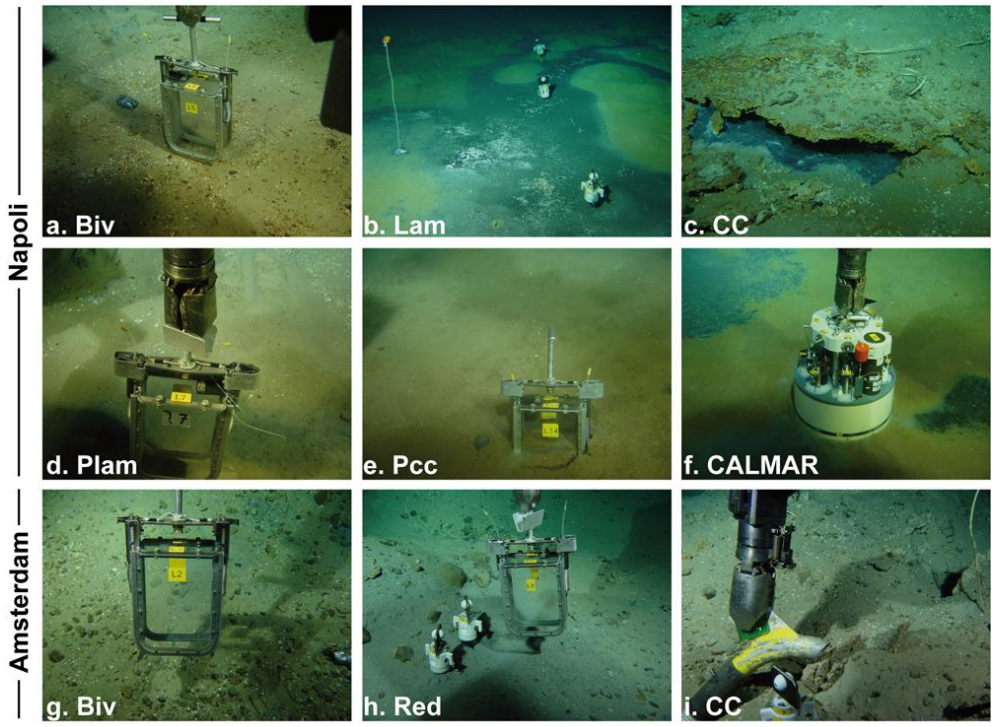


Figure 3. (a, b) Rarefaction curves and (c, d) the right tail-sum (RTS) intrinsic diversity profiles performed with macrofaunal abundances at the family level, for all the microhabitats, including the reference sites, sampled on the Napoli (a, c) and Amsterdam (b, d) mud volcanoes.

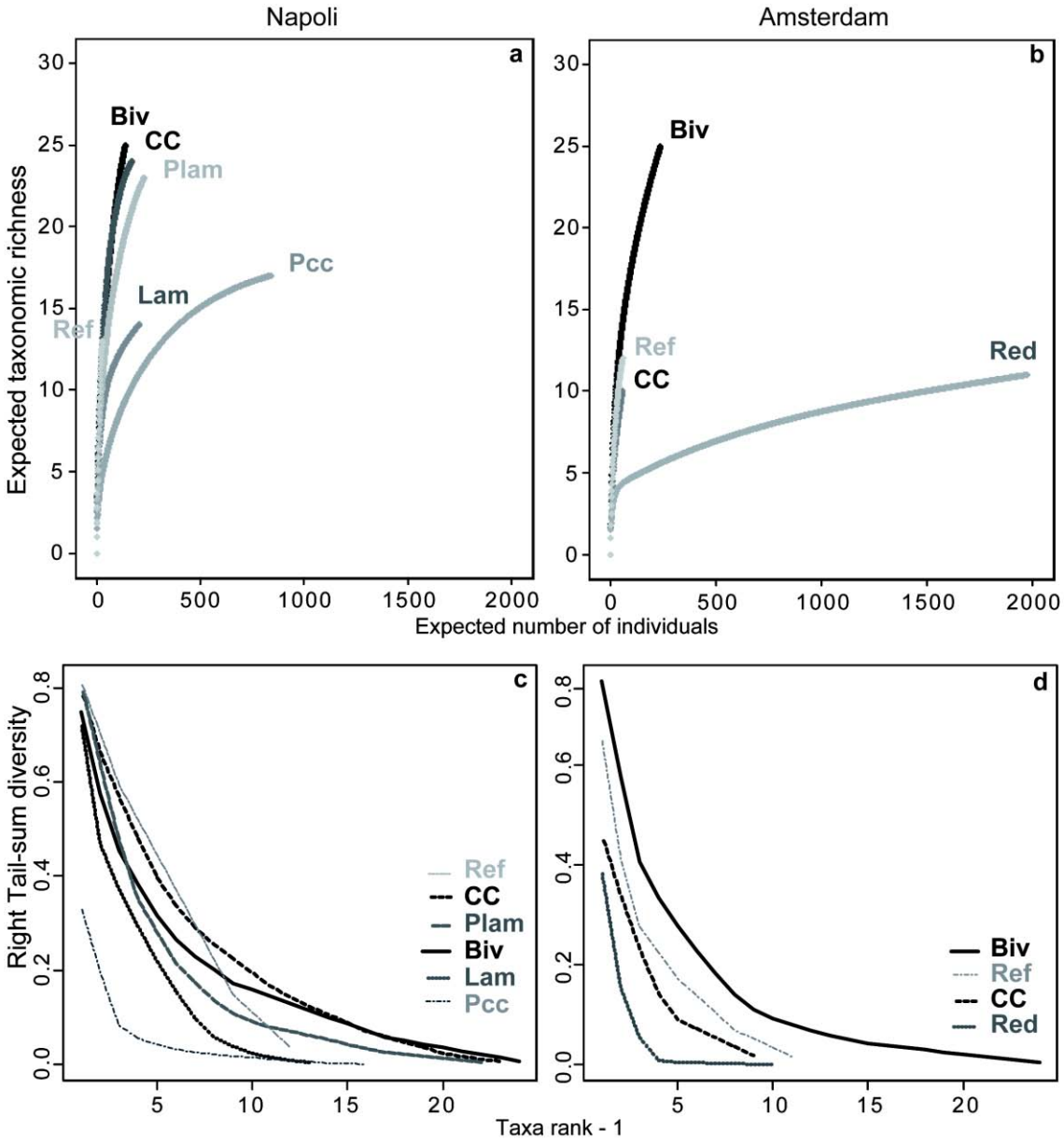


Figure 4. (a) Rarefaction curves and (b) the right tail-sum (RTS) intrinsic diversity profiles performed on macrofaunal abundances at the family level on the Napoli and Amsterdam mud volcanoes. Data from the active sites as well as the peripheral sites were pooled. The reference sites at each mud volcano were not included. Overall, Napoli, n = 17; Amsterdam, n = 9.

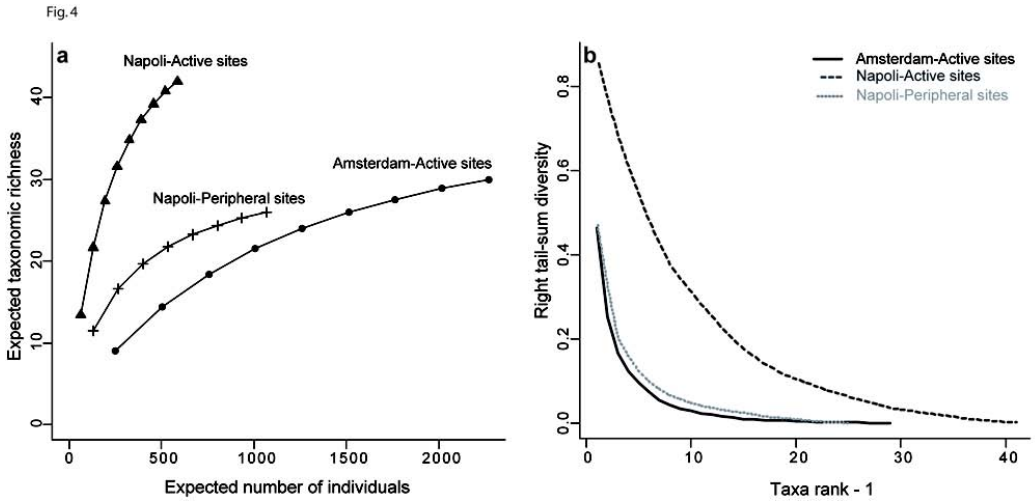


Figure 5. Density (individuals m^{-2}) of symbiont-bearing and heterotrophic macrofauna in each replicate of the microhabitats sampled on the Napoli and Amsterdam MVs. Biv = sediments with bivalve shells, Lam = *Lamellibrachia*, CC = carbonate crust, Plam = periphery of the Lamellibrachia, Pcc = periphery of the carbonate crust. Methane concentrations (black diamonds) for each replicate are given. The reduced microhabitats are shaded in grey (Lam and Red).

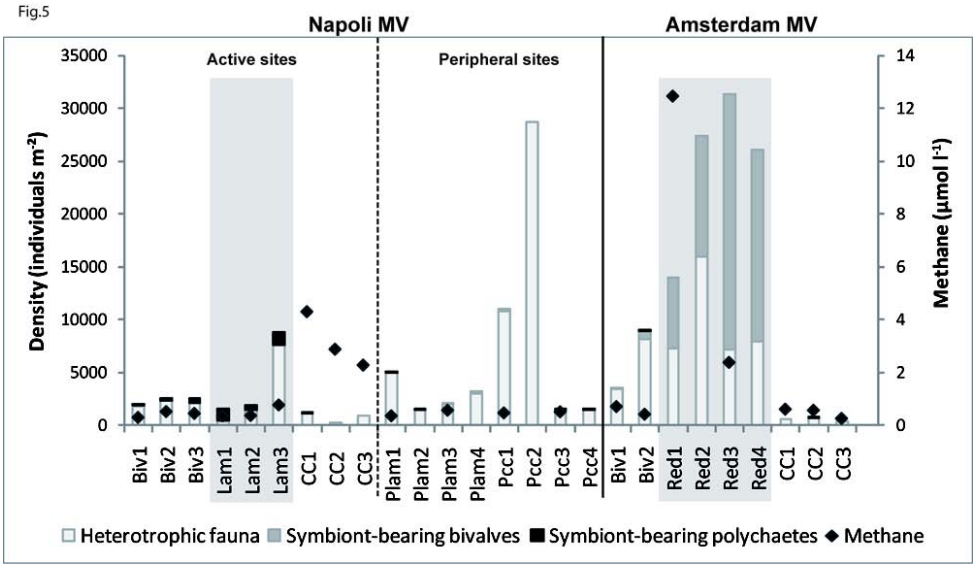


Figure 6. Principal component analysis (PCA, scaling type 1) of Hellinger transformed macrofaunal abundances with mixed taxonomic levels, on Napoli (a) Amsterdam (c) and on both MVs together (Mediterranean Ridge, e). The cercle of equilibrium contribution indicates the significant contribution of the taxa with arrows longer than the radius. Ward"s hierarchical clustering was performed on Hellinger transformed macrofaunal abundances for each microhabitat type on Napoli (b), Amsterdam (d) and both MVs (Mediterranean Ridge, f). Biv = bivalve shells, Lam = *Lamellibrachia*, CC = carbonate crusts, Plam = peripheral sediments in the vicinity of Lam, and Pcc = peripheral sediments in the vicinity of CC, Red=reduced sediments, Ref=reference site.

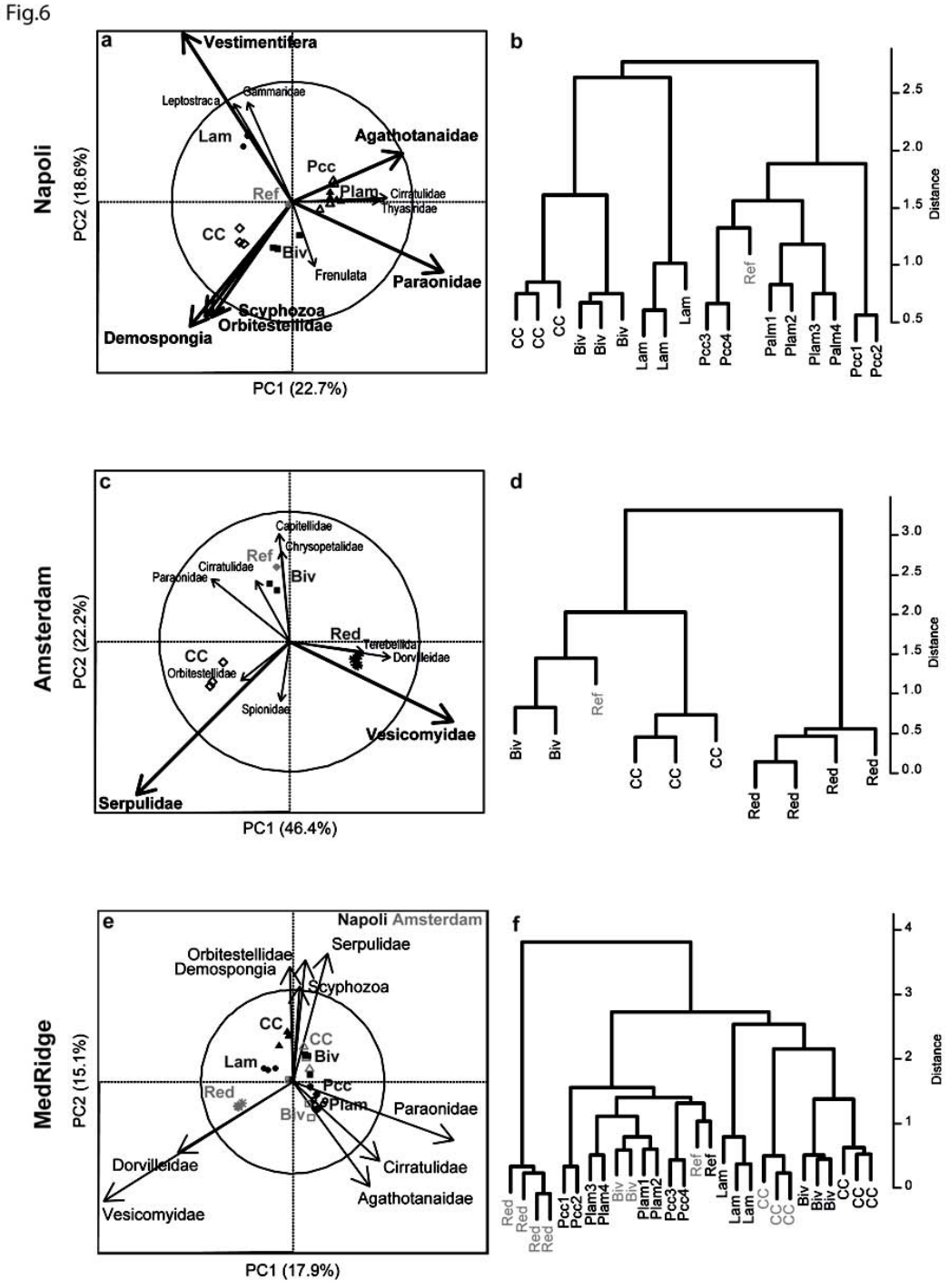


Figure 7. Canonical redundancy analysis (RDA, scaling type 2) performed on the matrix of macrofaunal abundances with mixed taxonomic levels sampled on Napoli (black) and on Amsterdam (grey) mud volcanoes and the matrix of environmental factors (black). The two first axes explain 56.4% of the total variance. Vectors are represented by arrows and centroïds by dots. Sed: soft sediments, Co: concretions.

